A methodology for the identification of physical parameters of soil-foundation-bridge pier systems from identified state-space models

A Methodology for the Identification of Physical Parameters of Soil-Foundation-Pier Systems from Identified State-Space Models

Carbonari S.[a1], Dezi F.[b], Arezzo D.[a], Gara F.[a]

[a] Department of Civil and Building Engineering, and Architecture, DICEA, Università Politecnica delle Marche, Via Brecce Bianche, 12, 60131 Ancona, Italy. E-mail: s.carbonari@univpm.it, d.arezzo@pm.univpm.it, f.gara@univpm.it

[b] Department of Economics, Science and law, DESD, University of San Marino, Via Consiglio dei Sessanta, 99, 47891, Republic of San Marino. E-mail: francesca.dezi@unirsm.sm

Abstract

A methodology for the identification of the physical parameters of a model describing the transverse dynamics of soil-foundation-pier systems founded on piles is presented in this paper, starting from identified state-space models of the systems obtained from results of dynamic experimental tests and identification techniques available in the literature. By assuming the order of the model to be compliant with that of a numerical one suitably developed to capture the dynamics of the bridge pier, the procedure allows the identification of the stiffness, mass and damping matrices of the analytical model from which the physical parameters of the real system (e.g. masses, pier stiffness matrix and soil-foundation impedance) can be extracted by directly comparing the components of the identified and analytical matrices. The procedure allows the direct definition of the numerical model that best fits the experimental data without the need of any model calibration, and permits the identification of the soil-foundation compliance taking into account its intrinsic frequency-dependent behaviour. Firstly, the dynamics of the analytical model is formulated adopting the continuous-time first-order state-space form. The model includes the frequency-dependent behaviour of the soil-foundation system through the

[1] Corresponding author, Department of Construction, Civil Engineering and Architecture, DICEA, Università Politecnica delle Marche, Via Brecce Bianche, 60131 Ancona, Italy - E-mail address: s.carbonari@univpm.it

introduction of a lumped parameter model able to reproduce the typical soil-foundation impedances of pile foundations. Then, an identification strategy of the physical parameters of a generic realistic soil-foundation-pier system is proposed starting from the discrete-time state-space model identified from dynamic tests. The procedure is illustrated with some applications, simulating results of forced vibration and ambient vibration tests executed on a known system whose parameters are then identified according to the proposed approach. The procedure revealed to be effective to identify the stiffness, mass and damping matrixes of the known system, and consequently its physical parameters.

Keywords: system identification; state-space models; forced vibration tests; ambient vibration tests.

1. Introduction

Dynamic tests are nowadays widely employed in civil engineering for the dynamic characterization of existing constructions with the aim of calibrating numerical models for retrofitting strategies [e.g. 1-6] or of monitoring the structural health by tracking possible changes in time of the dynamic properties, especially after earthquakes [e.g. 7-12]. In this framework, the identification of the physical parameters of a system, i.e. of the components of the stiffness, mass and damping matrices, is of great interest since it allows a direct comparison with the relevant values of a numerical model simulating the real structure. In this way, procedures aimed to the damage detection are simplified because it is possible the observation of the reduced terms of the identified stiffness matrix and consequently the identification of the structural members contributing to the degraded stiffness terms. Forced Vibration Tests (FVTs) or Ambient Vibration Tests (AVTs) are generally performed to characterise a dynamical system; the former requires the use of actuators or shakers (usually vibrodynes) while the latter exploits the ambient excitation coming from the wind, human activities and tremors due to micro seismic activity. In forced vibration tests, the structure is excited by a known input force at particular frequencies of interest through shakers [e.g. 13-14]; concerning bridges, it was found that excitation by shakers generally produce the best results for short- to medium-span bridges (spans shorter than 100 m) [e.g. 15-16]. In these tests, both the loading on the structure and the resulting responses are known, so that the structural

characteristics can be unambiguously determined due to the reduction of uncertainties related to data processing and collection [15]. These tests also allow achieving high signal-to-noise ratios in the response measurements. Ambient vibration tests are a useful alternative, successfully applied to a large variety of civil engineering structures ranging from short- to long-span bridges [e.g. 15, 17-18], to high-rise buildings, and dams.

As for the identification of the system physical parameters, the problem is quite simple from the second-order form of the equations of motion if input and output, including displacements, velocities, and accelerations are measured in all the degrees of freedom of the system [19]. However, for both tests, usually only acceleration measurements are performed due to the availability of accurate, low-noise and lightweight accelerometers. Consequently, velocities and displacements must be computed by integrating noisy signals, leading to a poor model identification [20]. In addition, the approach is almost unfeasible for AVTs, for which the input vibration is unknown, unless the input is estimated through a suitable strategy. Indeed, particular tests configuration can be included in the experimental campaign repeating AVTs with added masses in different positions of the structure in order to be able to estimate the scaling factors that normalise the identified mode shapes with respect to the mass [21], so that they can be adopted to reconstruct the receptance matrix and finally the input noise [22].

A more efficient approach for the identification of the system physical parameters exploits the first-order state-space form of the equation of motion, which can be identified without the need to integrate or differentiate noisy data [23]. State-space models can be identified through well-established procedures available in the literature, starting from input-output data obtained through dynamic experimental tests; in this framework, subspace identification methods demonstrated to be robust and reliable methodologies for the dynamic characterization of input-output dynamic systems [24]. An identified state-space model is usually in a transformed coordinate system and a transformation is generally needed to express it in the physical coordinates so that the state vector contains displacements and velocities, and the elements of the model are directly related to the stiffness, mass and damping matrices of the system [23]. Procedures for recovering stiffness, mass and damping matrices have been proposed in the

literature, differing each other for the grade of complexity, which in turn depends on the special coordinate systems in which the system has to be expressed [23, 25-28].

In this paper a methodology for the identification of the physical parameters of a model describing the transverse dynamics of Soil-Foundation-Pier (SFP) systems is presented, starting from identified state-space models obtained by processing the results of dynamic experimental tests. The order of the model is assumed to be compliant with that of a numerical model suitably developed to capture the dynamics of the bridge pier in the transverse direction and the identification of the system stiffness, mass and damping parameters of the analytical model is obtained by directly comparing components of the identified and analytical matrices. Consequently, the procedure allows the direct definition of the parameters of the numerical model that best fits the experimental data avoiding the use of any model calibration strategy. Firstly, the analytical model that has to be identified is presented and the continuous-time first-order state-space form of the equation of motion is formulated. The model accounts for the frequency-dependent soil-foundation system compliance, which may play an important role in the interpretation of dynamic tests on structures [29-30], through the introduction of Lumped Parameter Models (LPMs) [31-34] that are able to reproduce the typical soil-foundation impedances of pile foundations [33]. Then, an identification strategy of the physical parameters of a generic real soil-foundation-pier system is proposed generalising procedures available in the literature and referred to mechanical systems [23, 25-26] usually excited by actuators. The procedure applies to structural systems such as the SFP system investigated in this work, where not only FVTs but also (and more often) AVTs are performed. Starting from the discrete-time state-space model identified from dynamic tests through suitable strategies available in the literature [24], the stiffness, mass, and damping parameters of the analytical model are finally identified by directly comparing components of the identified and analytical matrices. Therefore, the methodology can be exploited for the structural health monitoring of the system and for the damage detection, by simply repeating tests during time and by identifying changes in the physical parameters of the structural system (e.g. the position of the observed degraded terms of the stiffness matrix may contribute to the identification of the damaged members), including the soil-

foundation system, where a direct damage observation is impossible. In addition, the approach allows the experimental identification of the soil-foundation compliance, expressed through a LPM able to reproduce the frequency-dependent behaviour of the soil-foundation system in time domain-analysis. Some numerical illustrations are finally presented, starting from results of two dynamic tests simulated on a known system. In detail, the response of the system subjected to a Gaussian white noise and to sinusoidal sweep signals is simulated and the system parameters, which are assumed to be a-priori known, are identified through the proposed approach in order to evaluate discrepancies between the known and identified quantities.

2 The proposed methodology

A methodology for the identification of the physical parameters of a model describing the transverse dynamics of real soil-foundation-pier systems is proposed in this section. The methodology is based on experimental data obtained from dynamic tests such as FVTs and AVTs, from which a first-order state-space model having order equal to that of the analytical predictive one is identified. The components of the stiffness, mass, and damping matrices of the analytical model is finally obtained, from which the physical parameters of the model are extracted. Stating the reliability of the interpreting model, the latter are representative of the real investigated system.

2.1 The soil-foundation-pier model

In this section, an analytical model for the interpretation of the measured dynamics of single bridge piers in the transverse direction is presented. With reference to pile foundations, the proposed model accounts for the soil-foundation system compliance assuming that its frequency-dependent stiffness can be well captured using a LPM. The latter is constituted by sets of springs, dashpot and masses with frequency-independent parameters suitably arranged and calibrated so that the impedance matrix of the LPM suits well that of the soil-foundation system in the frequency range of interest for practical applications (i.e. the range within which the resonance frequencies of the structures fall). In this paper, the model proposed

by Carbonari et al. [33] is used in view of its effectiveness in capturing the coupled roto-translational behaviour of pile foundations, which are typical for bridges, with a limited set of parameters.

The soil-foundation-pier system is depicted in Figure 1a while in Figure 1b the model proposed for the interpretation of its dynamics is shown. The soil-foundation compliance is taken into account through the above mentioned LPM, which is reported for clearness in Figure 1c with the relevant notation. The system is characterised by 5 degrees of freedom (*dof*), namely the translation u_f and rotation φ_f at the foundation level (node *f*), the translation u_p and φ_p of the top of the pier (node *p*), and the translation of the deck u_d (node *d*), which is connected to the pier cap through a spring of stiffness *k* in order to make the system also suitable for isolated bridges.

Masses of the deck m_d, of the pier cap m_c and of the foundation m_f are lumped at the centroids of the relevant members, while the pier mass m_p is assumed to be lumped at the pier ends. Furthermore, the foundation cap and the pier cap are assumed to be rigid while the pier is modelled as a Timoshenko beam. The geometric parameters of the system are reported in Figure 1a. The dynamic equilibrium equations of the system subjected to ambient accelerations or forced vibrations assumes the general form

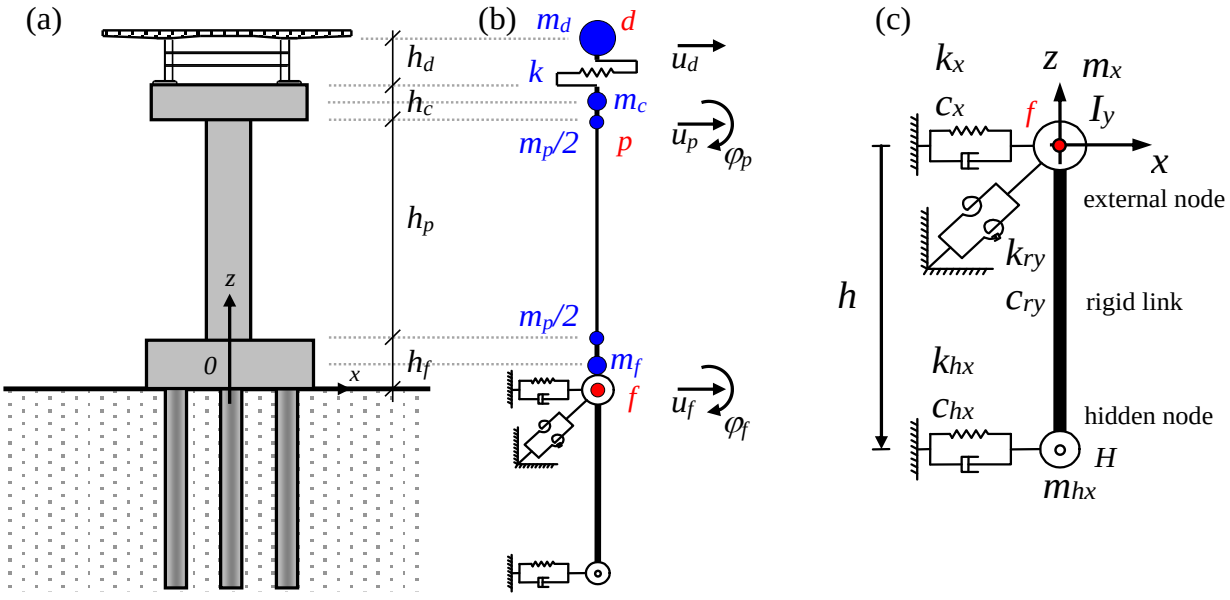

Figure 1. (a) Soil-foundation-pier system; (b) numerical model and (c) LPM with parameters speification.

$$(\mathbf{M}_s + \mathbf{M}_{LPM})\ddot{\mathbf{u}}(t) + (\mathbf{C}_s + \mathbf{C}_{LPM})\dot{\mathbf{u}}(t) + (\mathbf{K}_s + \mathbf{K}_{LPM})\mathbf{u}(t) = \mathbf{b}f(t) \tag{1}$$

where

$$\mathbf{u} = [u_d \quad u_p \quad \varphi_p \quad u_f \quad \varphi_f]^T \tag{2}$$

is the vector collecting displacements of the *dof* of the system, $\mathbf{M}_s$, $\mathbf{C}_s$ and $\mathbf{K}_s$ are the mass, damping and stiffness matrices of the superstructure, respectively, while $\mathbf{M}_{LPM}$, $\mathbf{C}_{LPM}$ and $\mathbf{K}_{LPM}$ are the mass, damping and stiffness matrices of the lumped system that accounts for the soil-foundation system compliance. The superstructure mass and stiffness matrices assume the form

$$\mathbf{M}_s = \begin{bmatrix} m_d & 0 & 0 & 0 & 0 \\ & m_c + \frac{m_p}{2} & m_c\frac{h_c}{2} & 0 & 0 \\ & & m_c\frac{h_c^2}{4} & 0 & 0 \\ & sym & & \frac{m_p}{2} + m_f & \frac{m_p}{2}h_f + m_f\frac{h_f}{2} \\ & & & & \frac{m_p}{2}h_f^2 + m_f\frac{h_f^2}{4} \end{bmatrix} \tag{3}$$

$$\mathbf{K}_s = \begin{bmatrix} k & -k & -k(h_c + h_d) & 0 & 0 \\ & k + \frac{12EJ}{h_p^3}\frac{1}{\mu} & k(h_c + h_d) - \frac{6EJ}{h_p^2}\frac{1}{\mu} & -\frac{12EJ}{h_p^3}\frac{1}{\mu} & -\frac{12EJ}{h_p^3}\frac{1}{\mu}\left(h_f + \frac{h_p}{2}\right) \\ & & k(h_c + h_d)^2 + \frac{3EJ}{h_p\mu} + \frac{EJ}{h_p} & \frac{6EJ}{h_p^2}\frac{1}{\mu} & \frac{6EJ}{h^2}\frac{1}{\mu}\left(h_f + \frac{h_p}{2}\right) - \frac{EJ}{h_p} \\ & sym & & \frac{12EJ}{h_p^3}\frac{1}{\mu} & \frac{12EJ}{h_p^3}\frac{1}{\mu}\left(h_f + \frac{h_p}{2}\right) \\ & & & & \frac{12EJ}{h_p^3}\frac{1}{\mu}\left(h_f^2 + h_p h_f + \frac{h_p^2}{4}\right) + \frac{EJ}{h_p} \end{bmatrix} \tag{4}$$

where E and J are the Young's modulus and the moment of inertia of the pier, respectively, and

$$\mu = 1 + 12\frac{\chi EJ}{GAh_p^2} \tag{5}$$

in which χ, G and A are the shear correction factor, the shear modulus of the pier material, and the area of the pier cross-section, respectively. The damping matrix of the superstructure is assumed to be proportional to both stiffness and mass, according to the Rayleigh approach, which provides

$$\mathbf{C}_s = \alpha \mathbf{M}_s + \beta \mathbf{K}_s \tag{6}$$

where coefficients α and β can be calibrated to get defined damping ratios in correspondence of two resonance frequencies of the structure. In addition, the mass, stiffness, and damping matrices of the LPM, which simulate the soil-foundation compliance, are

$$\mathbf{M}_{LPM} = \begin{bmatrix} 0 & 0 & 0 & 0 & 0 \\ & 0 & 0 & 0 & 0 \\ & & 0 & 0 & 0 \\ & sym & & m_x + m_{hx} & -m_{hx}h \\ & & & & I_y + m_{hx}h^2 \end{bmatrix} \tag{7}$$

$$\mathbf{K}_{LPM} = \begin{bmatrix} 0 & 0 & 0 & 0 & 0 \\ & 0 & 0 & 0 & 0 \\ & & 0 & 0 & 0 \\ & sym & & k_x + k_{hx} & -k_{hx}h \\ & & & & k_{ry} + k_{hx}h^2 \end{bmatrix} \tag{8}$$

$$\mathbf{C}_{LPM} = \begin{bmatrix} 0 & 0 & 0 & 0 & 0 \\ & 0 & 0 & 0 & 0 \\ & & 0 & 0 & 0 \\ & sym & & c_x + c_{hx} & -c_{hx}h \\ & & & & c_{ry} + c_{hx}h^2 \end{bmatrix} \tag{9}$$

Finally, in equations (1), **b** is the load influence vector. In case of forced vibration tests, **b** determines where the known force f is applied, while in case of ambient vibration tests, by assuming that the excitation only comes from the soil accelerations (i.e. neglecting the contribution of wind and vehicles on the bridge) $\ddot{u}_g$ (i.e. $f = \ddot{u}_g$),

$$\mathbf{b} = -\mathbf{M}_s \bar{\mathbf{b}} = \begin{bmatrix} m_d \\ m_c + \dfrac{m_p}{2} \\ m_c \dfrac{h_c}{2} \\ \dfrac{m_p}{2} + m_f \\ \dfrac{m_p}{2} h_f + m_f \dfrac{h_f}{2} \end{bmatrix} \qquad \bar{\mathbf{b}} = [1 \quad 1 \quad 0 \quad 1 \quad 0]^T \tag{10a,b}$$

where $\mathbf{c} = [\mathbf{1} \quad \mathbf{1} \quad \mathbf{0} \quad \mathbf{1} \quad \mathbf{0}]^{\boldsymbol{T}}$ is an influence vector determining the *dofs* where the ground acceleration acts. It is worth observing that the mass matrix in the previous equation only includes the superstructure masses [35].

2.2 The continuous-time state-space model

The first-order continuous-time state-space model is obtained by introducing the state vector

$$\mathbf{v} = \begin{bmatrix} \mathbf{u} \\ \dot{\mathbf{u}} \end{bmatrix} \tag{11}$$

that allows expressing the second-order equation (1) as

$$\mathbf{P}\dot{\mathbf{v}} + \mathbf{Q}\mathbf{v} = \mathbf{\Gamma} f \tag{12}$$

where

$$\mathbf{P} = \begin{bmatrix} \mathbf{C} & \mathbf{M} \\ \mathbf{M} & \mathbf{0} \end{bmatrix} \qquad \mathbf{Q} = \begin{bmatrix} \mathbf{K} & \mathbf{0} \\ \mathbf{0} & -\mathbf{M} \end{bmatrix} \qquad \mathbf{\Gamma} = \begin{bmatrix} \mathbf{b} \\ \mathbf{0} \end{bmatrix} \tag{13a,b,c}$$

By pre-multiplying equation (12) by $\mathbf{P}^{-1}$, the following state equation can be obtained

$$\dot{\mathbf{v}} = \mathbf{A}_c \mathbf{v} + \mathbf{B}_c f \tag{14}$$

where

$$\mathbf{A}_c = \begin{bmatrix} \mathbf{0} & \mathbf{I} \\ -\mathbf{M}^{-1}\mathbf{K} & -\mathbf{M}^{-1}\mathbf{C} \end{bmatrix} \qquad \mathbf{B}_c = \begin{bmatrix} \mathbf{0} \\ \mathbf{M}^{-1}\mathbf{b} \end{bmatrix} \tag{15a,b}$$

in which

$$\mathbf{M} = \mathbf{M}_s + \mathbf{M}_{LPM} \qquad \mathbf{K} = \mathbf{K}_s + \mathbf{K}_{LPM} \qquad \mathbf{C} = \mathbf{C}_s + \mathbf{C}_{LPM} \tag{16a,b,c}$$

and $\mathbf{I}$ is the identity matrix of order 5. In modern control theory equation (14) is used together with the following observation equation to express system (1) in the form of a continuous-time state-space model:

$$\mathbf{y} = \mathbf{D}_c \mathbf{v} + \mathbf{E}_c f \tag{17}$$

By assuming that the observation equation includes all the set of accelerations at the *dofs* (this assumption will be clear in the next section where the analytical model is compared with a real system

in which accelerations are measured) the following expressions hold for the output matrix $\mathbf{D}_c \in \mathbb{R}^{5x10}$ and for the transmission matrix $\mathbf{E}_c \in \mathbb{R}^{5x1}$:

$$\mathbf{D}_c = [-\mathbf{M}^{-1}\mathbf{K} \quad -\mathbf{M}^{-1}\mathbf{C}] \qquad \mathbf{E}_c = \mathbf{M}^{-1}\mathbf{b} \tag{18a,b}$$

It must be remarked that if the input is constituted by forces, the observed accelerations are absolute, as those registered in the real system through instrumentations during tests; on the contrary, if the input is represented by soil accelerations, Eq. (17) provides accelerations relative to the ground. Thus, in order to get the absolute accelerations if $f = \ddot{u}_g$, Eq (18b) should be substituted with

$$\mathbf{E}_c = \mathbf{M}^{-1}\mathbf{b} + \bar{\mathbf{b}} \tag{18c}$$

It can be remarked that the eigenvalue problem associated to (12) is

$$\mathbf{P}\boldsymbol{\psi}\boldsymbol{\Lambda} + \mathbf{Q}\boldsymbol{\psi} = \mathbf{0} \tag{19}$$

where $\boldsymbol{\psi} \in \mathbb{C}^{10x10}$ contains the complex eigenvectors as columns and $\boldsymbol{\Lambda} \in \mathbb{C}^{10x10}$ is a diagonal matrix containing the 10 complex eigenvalues λ_i (i = 1…10). For a structure in which the radiation damping of the soil-foundation system is taken into account, a stable system is expected, and the eigenvalues are either complex-valued with negative real parts or negative real-valued. If the eigenvalue is complex-valued, the relevant eigenvector is also complex and corresponds to an under-damped vibration mode; if the eigenvalues are real-valued, the corresponding eigenvectors are real, and modes are over-damped. Also, all the complex eigenvalues and eigenvectors appear in complex-conjugate pairs, while each over-damped mode can be considered as an independent basic unit. If $n_c \leq 5$ is the number of pairs of complex eigenvalues, they appear in the form

$$\lambda_c, \lambda_c^* = -\xi_c\omega_c \pm j\omega_c\sqrt{1-\xi_c^2} \qquad c=1\ldots n_c \tag{20}$$

in which ξ_i and ω_i are the i-th damping ratio and resonance frequency of the corresponding undamped system. By individually handling the real $n_r = 10 - 2n_c$ eigenvalues, they appear in the form

$$\lambda_r = -\omega_r \qquad r=1\ldots n_r \tag{21}$$

Thus, it can be shown that $\boldsymbol{\psi}$ and $\boldsymbol{\Lambda}_c$ have the following layouts

$$\boldsymbol{\psi} = \begin{bmatrix} \boldsymbol{\varphi}_c & \boldsymbol{\varphi}_c^* & \boldsymbol{\varphi}_r \\ \boldsymbol{\varphi}_c\boldsymbol{\Lambda}_c & \boldsymbol{\varphi}_c^*\boldsymbol{\Lambda}_c^* & \boldsymbol{\varphi}_r\boldsymbol{\Lambda}_r \end{bmatrix}_{10x10} \qquad \boldsymbol{\Lambda} = \begin{bmatrix} \boldsymbol{\Lambda} & \mathbf{0} & \mathbf{0} \\ \mathbf{0} & \boldsymbol{\Lambda}^* & \mathbf{0} \\ \mathbf{0} & \mathbf{0} & \boldsymbol{\Lambda}_r \end{bmatrix}_{10x10} \tag{22a,b}$$

where $\boldsymbol{\varphi}$ and $\boldsymbol{\Lambda}$ are the eigenvectors and eigenvalues of the second order system (1).

It can be proven that [30]

$$\mathbf{A}_c = \boldsymbol{\psi}\boldsymbol{\Lambda}\boldsymbol{\psi}^{-1} \tag{23}$$

which implies that $\boldsymbol{\Lambda}$ contains the eigenvalues and $\boldsymbol{\psi}$ the eigenvectors of $\mathbf{A}_c$. Consequently, matrix $\mathbf{A}_c$ can be used instead of **P** and **Q** to solve the eigenvalue problem.

2.3 Identification of the discrete-time state-space model for the real soil-foundation-pier system

Let we assume that dynamic tests are performed on a real soil-foundation-pier system to study its transverse dynamics and that its dynamics can be well represented by the above presented analytical interpreting model. Measurements are usually taken at discrete time instants k spaced by the time interval Δt. Usually, accelerations are measured due to the availability of accurate and lightweight accelerometers and the sensors layout must be conceived to make it possible obtaining accelerations relevant to the *dofs* of the above described system. A possible sensor layout, which assures such condition, is shown in Figure 2. Starting from the measured accelerations, those associated to the *dofs* of the analytical model are computed; for the example shown in Figure 2, the following transformation holds

$$\begin{bmatrix} u_d \\ u_p \\ \varphi_p \\ u_f \\ \varphi_f \end{bmatrix}_{exp} = \begin{bmatrix} 0 & 0 & 0 & 0 & 0 & 0 & 1 \\ 0 & 0 & 0 & 1 & -\frac{h_c}{l_c} & \frac{h_c}{l_c} & 0 \\ 0 & 0 & 0 & 0 & \frac{h_c}{l_c} & -\frac{h_c}{l_c} & 0 \\ 1 & -\frac{h_f}{l_f} & \frac{h_f}{l_f} & 0 & 0 & 0 & 0 \\ 0 & \frac{h_f}{l_f} & -\frac{h_f}{l_f} & 0 & 0 & 0 & 0 \end{bmatrix} \begin{bmatrix} U_f \\ V_{lf} \\ V_{rf} \\ U_c \\ V_{lc} \\ V_{rc} \\ U_d \end{bmatrix} \tag{24}$$

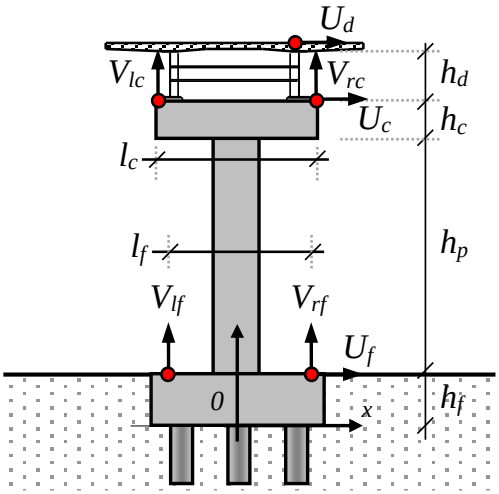

Figure 2. Sensor layout on a real soil-foundation-pier system.

Depending on the performed dynamic tests, the input actions can be known or not; the following three situations are herein considered and addressed below within the proposed procedure:

1. forced vibration tests are performed through the use of a vibrodyne acting on one degree of freedom of the system (i.e. at the deck or the foundation level);
2. ambient vibration tests are executed by measuring the ambient excitation coming from the ground (e.g. through the use of geophones);
3. ambient vibration tests are executed without measuring the ambient excitation.

Anyway, a general expression of the discrete-time state-space model has the following form:

$$\mathbf{v}_{k+1} = \mathbf{A}_d \mathbf{v}_k + \mathbf{B}_d \mathbf{g}_k + \boldsymbol{w}_k \tag{25a}$$

$$\mathbf{y}_k = \mathbf{D}_d \mathbf{v}_k + \mathbf{E}\mathbf{g}_k + \boldsymbol{v}_k \tag{25b}$$

where $\mathbf{v}_k = \mathbf{v}(k\Delta t)$ is the discrete-time state vector which contains the sampled displacements and velocities, $\mathbf{g}_k$ is the sampled input, and $\boldsymbol{w}_k$ and $\boldsymbol{v}_k$ are zero mean vector signals accounting for process noise due to disturbances and modelling inaccuracies and due to sensor inaccuracies, respectively. In the observation equation, $\mathbf{y}_k$ are the outputs and matrix $\mathbf{D}_d$ is the output matrix that extracts the observed *dofs* from the whole system. Obviously, if only the vibration of the structure is measured, it is impossible to distinguish, from an identification point of view, between the term $\mathbf{g}_k$ and the noise terms. Depending

on the performed tests, input-output or output-only techniques can be used for the state-space model identification and the evaluation of the modal parameters; however, if ambient vibration tests are performed without measuring the ground noise, matrices $\mathbf{B}_d$ and $\mathbf{E}$ cannot be identified. In this case, an indirect load estimation must be performed to proceed with the proposed methodology.

The load estimation is possible starting from the computation of the receptance matrix of the system, namely the matrix containing the Frequency Response Functions (FRF) between nodal displacements and nodal forces, expressed in terms of the modal parameters and poles obtained from the Operational Modal Analysis (OMA) [24]. The problem can be easily addressed in the frequency domain through the following equation:

$$\mathbf{V}(\omega) = -\omega^2 \mathbf{H}(\omega)\mathbf{F}(\omega) \tag{26}$$

where $\mathbf{V}(\omega)$ is the Fourier Transform of the measured accelerations and

$$\mathbf{H}(\omega) = \sum_{c=1}^{n_c} \left(\frac{Q_c \varphi_c \varphi_c^T}{j\omega - \lambda_c} + \frac{Q_c^* \varphi_c^* \varphi_c^{*H}}{j\omega - \lambda_c^*} \right) \tag{27}$$

where *H* denotes the Hermitian transpose. In equation (27) φ_c and λ_c are the *c*-th un-scaled mode shape and eigenvalue, respectively, obtained from the OMA. In addition,

$$Q_c = \frac{\gamma_c^2}{2j|\lambda_c|} \tag{28}$$

is a factor accounting for the scale of the mode φ_c. In equation (28) γ_c is the scaling factor of the *c*-th mode that allows obtaining the mass normalised mode shape from the un-scaled one. When OMA is performed, forces are not measured, the modal participation factors cannot be determined and the mode shape vectors cannot be scaled. However, different methods have been proposed recently to estimate the scaling factors involving repeated testing in which mass changes are introduced in the points where the mode shapes are known [21]. Thanks to these appraoches, scaling factors can be computed by performing a controlled mass addition experiments on the tested structure.

Starting from equation (26) the loads can be computed in the frequency domain according to

$$\mathbf{F}(\omega) = -\frac{\mathbf{H}^{-1}(\omega)\mathbf{V}(\omega)}{\omega^2} \tag{29}$$

and the relevant counterpart of input signals in the time domain can be evaluated through an Inverse Fourier Transform. It is worth noting that if this approach is adopted, estimated forces acting on the structure are those deriving from the overall ambient excitation, including tremors, wind, traffic and human activities in general.

Once the loads acting on the structure are definitively known, an input-output identification can be performed by assuming the model to be of the same order of the analytical one proposed in the previous section, in order to assure that matrix $\mathbf{A}_d$ and $\mathbf{A}_c$ as well as $\mathbf{D}_d$ and $\mathbf{D}_c$ have the same dimensions. However, despite the latter have the same rank, they may be substantially different because they refer to a discrete and a continuous system, respectively, and because the state-space model representation is not unique. Indeed, the set ($\mathbf{A}_{ph}$, $\mathbf{B}_{ph}$, $\mathbf{D}_{ph}$) in physical coordinates is equal to that of a set ($\mathbf{A}_r$, $\mathbf{B}_r$, $\mathbf{D}_r$) = ($\overline{\mathbf{T}}\mathbf{A}_{ph}\overline{\mathbf{T}}^{-1}$, $\overline{\mathbf{T}}\mathbf{B}_{ph}$, $\mathbf{D}_{ph}\overline{\mathbf{T}}^{-1}$) where $\overline{\mathbf{T}}$ is any invertible transformation that changes the set of coordinates. Thus, after converting the identified discrete state-space model ($\mathbf{A}_d$, $\mathbf{B}_d$, $\mathbf{D}_d$) to the relevant continuous-time representation ($\mathbf{A}_r$, $\mathbf{B}_r$, $\mathbf{D}_r$) (this is possible if the sampling interval Δt is sufficiently small to prevent aliasing [23, 36]), the latter is not in the physical coordinates unless a suitable transformation $\mathbf{T}$ is applied. The transformation $\mathbf{T}$ that allows converting the identified state-space model into the physical coordinates can be determined through different approaches that depend on the measured quantities. In the sequel, the case that assumes the full set of accelerations available is addressed. The system matrix in the physical coordinates can be obtained according to the following transformation:

$$\mathbf{A}_{ph} = \mathbf{T}\mathbf{A}_r\mathbf{T}^{-1} \tag{30a}$$

$$\mathbf{B}_{ph} = \mathbf{T}\mathbf{B}_r \tag{30b}$$

$$\mathbf{D}_{ph} = \mathbf{D}_r \mathbf{T}^{-1} \tag{30c}$$

Taking into account the layout of matrices appearing in equation (18a) and (15a), and suitably partitioning matrix $\mathbf{T}$, and $\mathbf{D}_r$, the following conditions can be imposed for the evaluation of the transformation $\mathbf{T}$:

$$\begin{bmatrix} -\mathbf{M}^{-1}\mathbf{K} & -\mathbf{M}^{-1}\mathbf{C} \end{bmatrix} \begin{bmatrix} \mathbf{T}_{11} & \mathbf{T}_{12} \\ \mathbf{T}_{21} & \mathbf{T}_{22} \end{bmatrix} = \begin{bmatrix} \mathbf{D}_{r11} & \mathbf{D}_{r12} \end{bmatrix} \tag{31a}$$

$$\begin{bmatrix} \mathbf{T}_{11} & \mathbf{T}_{12} \\ \mathbf{T}_{21} & \mathbf{T}_{22} \end{bmatrix} \begin{bmatrix} \mathbf{A}_{r11} & \mathbf{A}_{r12} \\ \mathbf{A}_{r21} & \mathbf{A}_{r22} \end{bmatrix} = \begin{bmatrix} \mathbf{0} & \mathbf{I} \\ -\mathbf{M}^{-1}\mathbf{K} & -\mathbf{M}^{-1}\mathbf{C} \end{bmatrix} \begin{bmatrix} \mathbf{T}_{11} & \mathbf{T}_{12} \\ \mathbf{T}_{21} & \mathbf{T}_{22} \end{bmatrix} = \begin{bmatrix} \mathbf{T}_{21} & \mathbf{T}_{22} \\ \mathbf{D}_{r11} & \mathbf{D}_{r12} \end{bmatrix} \tag{31b}$$

Equation (31b) provides a system of four equations in the unknowns $\mathbf{T}_{11}$, $\mathbf{T}_{12}$, $\mathbf{T}_{13}$, $\mathbf{T}_{14}$, from which components of matrix $\mathbf{T}$ can be obtained as follows:

$$\begin{bmatrix} \mathbf{T}_{11} \\ \mathbf{T}_{12} \\ \mathbf{T}_{21} \\ \mathbf{T}_{22} \end{bmatrix} = \begin{bmatrix} \mathbf{A}_{r11} & \mathbf{A}_{r21} & -\mathbf{I} & \mathbf{0} \\ \mathbf{A}_{r12} & \mathbf{A}_{r22} & \mathbf{0} & -\mathbf{I} \\ \mathbf{0} & \mathbf{0} & \mathbf{A}_{r11} & \mathbf{A}_{r22} \\ \mathbf{0} & \mathbf{0} & \mathbf{A}_{r12} & \mathbf{A}_{r22} \end{bmatrix}^{-1} \begin{bmatrix} \mathbf{0} \\ \mathbf{0} \\ \mathbf{D}_{r11} \\ \mathbf{D}_{r12} \end{bmatrix} \tag{32}$$

Once the trasformation $\mathbf{T}$ is computed, equations (30) can be used to compute the system matrix in the physical coordinates. Extracting the stiffness, mass and damping matrices from the state-space model in physical coordinates is now a linear problem; by recognising that the layout of matrices $\mathbf{A}_{ph}$ and $\mathbf{B}_{ph}$ is

$$\mathbf{A}_{ph} = \begin{bmatrix} \mathbf{0} & \mathbf{I} \\ -\mathbf{X} & -\mathbf{Y} \end{bmatrix} \qquad \mathbf{B}_{ph} = \begin{bmatrix} \mathbf{0} \\ \boldsymbol{Z} \end{bmatrix} \tag{33a,b}$$

the linear problem can be formulated as

$$\mathbf{X} = \mathbf{M}^{-1}\mathbf{K} \qquad \mathbf{Y} = \mathbf{M}^{-1}\mathbf{C} \qquad \mathbf{Z} = \mathbf{M}^{-1}\mathbf{b} \tag{34a,b,c}$$

However, the above equations are not sufficient to compute $\mathbf{M}$, $\mathbf{K}$ and $\mathbf{C}$ if $\mathbf{b}$ is not square and full rank (as almost always occurs since forces are never applied at all the degrees of freedom) and further equations must be added exploting the symmetry properties of matrices $\mathbf{M}$, $\mathbf{K}$ and $\mathbf{C}$, which allow writing

$$\mathbf{M}\mathbf{X} = \mathbf{X}^T\mathbf{M} \qquad \mathbf{M}\mathbf{Y} = \mathbf{Y}^T\mathbf{M} \tag{35a,b}$$

By defining a stack operator *S* (i.e. an operator that produces a vector by lining up columns of the matrix to which it is applied) and remembering the identity $(\mathbf{UVW})^S = (\mathbf{W}^T \otimes \mathbf{U})\mathbf{V}^S$, the following conditions hold:

$$\mathbf{K}^S = (\mathbf{X}^T \otimes \mathbf{I})\mathbf{M}^S \tag{36a}$$

$$\mathbf{C}^S = (\mathbf{Y}^T \otimes \mathbf{I})\mathbf{M}^S \tag{36b}$$

$$\mathbf{b}^S = (\mathbf{Z}^T \otimes \mathbf{I})\mathbf{M}^S \tag{36c}$$

$$(\mathbf{X}^T \otimes \mathbf{I})\mathbf{M}^S = (\mathbf{I} \otimes \mathbf{X}^T)\mathbf{M}^S \tag{36d}$$

$$(\mathbf{Y}^T \otimes \mathbf{I})\mathbf{M}^S = (\mathbf{I} \otimes \mathbf{Y}^T)\mathbf{M}^S \tag{36e}$$

where $\mathbf{I}$ is a 5x5 identity matrix and $\otimes$ is the Kronecker product. Equations (36) can be re-arranged in the following system

$$\begin{bmatrix} \mathbf{X}^T \otimes \mathbf{I} & \mathbf{0} & -\mathbf{I} \\ \mathbf{Y}^T \otimes \mathbf{I} & -\mathbf{I} & \mathbf{0} \\ (\mathbf{Z}^T \otimes \mathbf{I}) & \mathbf{0} & \mathbf{0} \\ (\mathbf{X}^T \otimes \mathbf{I}) - (\mathbf{I} \otimes \mathbf{X}^T) & \mathbf{0} & \mathbf{0} \\ (\mathbf{Y}^T \otimes \mathbf{I}) - (\mathbf{I} \otimes \mathbf{Y}^T) & \mathbf{0} & \mathbf{0} \end{bmatrix} \begin{bmatrix} \mathbf{M}^S \\ \mathbf{C}^S \\ \mathbf{K}^S \end{bmatrix} = \begin{bmatrix} \mathbf{0} \\ \mathbf{0} \\ \mathbf{b}^S \\ \mathbf{0} \\ \mathbf{0} \end{bmatrix} \tag{37}$$

System (37) can be solved in the least square sense to compute components of the mass, damping and stiffness matrices of the system if vector **b** is known, namely if FVTs are performed and the positions at which forces are applied on the structure are known. If the excitation is represented by the ambient noise coming from the ground, **b** depends on the unknowns, as evident from equation (10), unless forces are estimated through the recontruction of the receptance matrix starting from a set of AVTs and OMA performed on the system. Anyway, if accelerations exciting the structure at the ground level are measured during AVTs, the following system can be assembled

$$\begin{bmatrix} \mathbf{X}^T \otimes \mathbf{I} & \mathbf{0} & -\mathbf{I} \\ \mathbf{Y}^T \otimes \mathbf{I} & -\mathbf{I} & \mathbf{0} \\ (\mathbf{Z}^T \otimes \mathbf{I}) - \mathbf{R} & \mathbf{0} & \mathbf{0} \\ (\mathbf{X}^T \otimes \mathbf{I}) - (\mathbf{I} \otimes \mathbf{X}^T) & \mathbf{0} & \mathbf{0} \\ (\mathbf{Y}^T \otimes \mathbf{I}) - (\mathbf{I} \otimes \mathbf{Y}^T) & \mathbf{0} & \mathbf{0} \end{bmatrix} \begin{bmatrix} \mathbf{M}^S \\ \mathbf{C}^S \\ \mathbf{K}^S \end{bmatrix} = \begin{bmatrix} \mathbf{0} \\ \mathbf{0} \\ \mathbf{0} \\ \mathbf{0} \\ \mathbf{0} \end{bmatrix} \tag{38}$$

where, taking into account equation (10),

$$\mathbf{R} = \begin{bmatrix} 1 & \mathbf{0}_{1x5} & 0 & 0 & \mathbf{0}_{1x10} & 0 & 0 & \mathbf{0}_{1x5} \\ 0 & \mathbf{0}_{1x5} & 1 & 0 & \mathbf{0}_{1x10} & 0 & 0 & \mathbf{0}_{1x5} \\ 0 & \mathbf{0}_{1x5} & 0 & 1 & \mathbf{0}_{1x10} & 0 & 0 & \mathbf{0}_{1x5} \\ 0 & \mathbf{0}_{1x5} & 0 & 0 & \mathbf{0}_{1x10} & 1 & 0 & \mathbf{0}_{1x5} \\ 0 & \mathbf{0}_{1x5} & 0 & 0 & \mathbf{0}_{1x10} & 0 & 1 & \mathbf{0}_{1x5} \end{bmatrix} \tag{39}$$

A non-trivial solution of the system can be found in this case avoiding the need of estimating forces acting on the structure through the receptance matrix (i.e. avoiding the need of repeting AVTs by adding some masses on the structure in different posistions and repeating tests and OMAs) by assuming for example the mass of the deck m_d to be known. This allows formulating the following linear system of equations

$$\begin{bmatrix} \cup_{2:25}^{all} (\mathbf{X}^T \otimes \mathbf{I}) & \mathbf{0} & -\mathbf{I} \\ \cup_{2:25}^{all} (\mathbf{Y}^T \otimes \mathbf{I}) & -\mathbf{I} & \mathbf{0} \\ \cup_{2:25}^{all} [(\mathbf{Z}^T \otimes \mathbf{I}) + \mathbf{R}] & \mathbf{0} & \mathbf{0} \\ \cup_{2:25}^{all} [(\mathbf{X}^T \otimes \mathbf{I}) - (\mathbf{I} \otimes \mathbf{X}^T)] & \mathbf{0} & \mathbf{0} \\ \cup_{2:25}^{all} [(\mathbf{Y}^T \otimes \mathbf{I}) - (\mathbf{I} \otimes \mathbf{Y}^T)] & \mathbf{0} & \mathbf{0} \end{bmatrix} \begin{bmatrix} \cup_{1}^{2:25} \mathbf{M}^S \\ \mathbf{C}^S \\ \mathbf{K}^S \end{bmatrix} = m_d \begin{bmatrix} \cup_{all}^{1:1} (\mathbf{X}^T \otimes \mathbf{I}) \\ \cup_{all}^{1:1} (\mathbf{Y}^T \otimes \mathbf{I}) \\ \cup_{all}^{1:1} [(\mathbf{Z}^T \otimes \mathbf{I}) + \mathbf{R}] \\ \cup_{all}^{1:1} [(\mathbf{X}^T \otimes \mathbf{I}) - (\mathbf{I} \otimes \mathbf{X}^T)] \\ \cup_{all}^{1:1} [(\mathbf{Y}^T \otimes \mathbf{I}) - (\mathbf{I} \otimes \mathbf{Y}^T)] \end{bmatrix} \tag{40}$$

where $\cup_{k:l}^{i:j}$ is an operator extracting rows from *i* to *j* and columns from *k* to *l* from the matrix to which it is applied.

2.4 Calculation of the stiffness, mass, and damping parameters of the analytical model

Once matrices **M**, **K** and **C** are determined, the stiffness, mass, and damping parameters of the system can be computed by comparing analytical terms of the matrices with the identified ones. In detail, the translational stiffness of the bridge support devices is

$$k = \mathbf{K}_{1,1} \tag{41}$$

while the stiffness matrix of the pier $\mathbf{K}_p$, which governs relationship between the top (p) and base (b) displacements collected in the vector $[u_p \quad \varphi_p \quad u_b \quad \varphi_b]^T$ and the shear forces (V) and bending moments (M) collected in the vector $[V_p \quad M_p \quad V_b \quad M_p]^T$ can be determined from

$$\mathbf{K}_p = \begin{bmatrix} \mathbf{K}_{2,2} - \mathbf{K}_{1,1} & \mathbf{K}_{2,3} + \mathbf{K}_{1,3} & \mathbf{K}_{1,1} - \mathbf{K}_{2,2} & \mathbf{K}_{2,3} + \mathbf{K}_{1,3} \\ & \mathbf{K}_{3,3} + \mathbf{K}_{1,3}(h_c + h_d) & -\mathbf{K}_{2,3} - \mathbf{K}_{1,3} & \mathbf{K}_{3,5} + (\mathbf{K}_{2,3} + \mathbf{K}_{1,3})h_f \\ & & \mathbf{K}_{2,2} - \mathbf{K}_{1,1} & -\mathbf{K}_{2,3} - \mathbf{K}_{1,3} \\ sym & & & \mathbf{K}_{3,3} + \mathbf{K}_{1,3}(h_c + h_d) \end{bmatrix} \tag{42}$$

by assuming the geometric parameters to be known (or measurable). As for the masses, the mass deck, if not assumed to be known during the identification procedure, can be determined through

$$m_d = \mathbf{M}_{1,1} \tag{43a}$$

while the remaining masses of the superstructure (i.e. of the pier cap and of the pier) can be computed through

$$m_c = \frac{2}{h_c}\mathbf{M}_{2,3} \tag{43b}$$

$$m_p = 2\left(\mathbf{M}_{2,2} - \frac{2}{h_c}\mathbf{M}_{2,3}\right) \tag{43c}$$

Unfortunately, the remaining three equalities between components of the identified and analytical mass matrices do not allow the computation of the foundation mass and the masses of the LPM (four unknowns). However, it can be reasonable to assume that the foundation mass m_f can be easily estimated from the design drawings of the structure and the density of the material, so that the masses of the LPM can be determined.

Above assumption on the foundation mass, make it possible to fully estimate parameters of the LPM. This means that the soil-foundation impedance matrix, approximated through the LPM, can be estimated starting from a dynamic experimental investigation on the real structure. Considering the well-recognised role of soil-structure interaction effects on the seismic response of structures, especially

bridges [37-42], the proposed procedure makes it possible to experimentally estimate the soil-foundation impedance matrix for a real SFP system.

In detail, the following equations hold for the stiffness parameters of the LPM:

$$k_x = \mathbf{K}_{4,4} - \frac{1}{h}\left[\left(\mathbf{K}_{2,2} - \mathbf{K}_{1,1}\right)\left(h + h_f + \frac{h_p}{2}\right) - \mathbf{K}_{4,5}\right] \tag{44a}$$

$$k_{hx} = \frac{1}{h}\left[\left(\mathbf{K}_{2,2} - \mathbf{K}_{1,1}\right)\left(h_f + \frac{h_p}{2}\right) - \mathbf{K}_{4,5}\right] \tag{44b}$$

$$\begin{aligned} k_{ry} = {} & \mathbf{K}_{5,5} + \mathbf{K}_{3,5} - \mathbf{K}_{3,4}\left(h_f + \frac{h_p}{2}\right) \\ & - h\left[\left(\mathbf{K}_{2,2} - \mathbf{K}_{1,1}\right)\left(h_f + \frac{h_p}{2} + \frac{h_f^2}{h} + \frac{h_p h_f}{h} + \frac{h_p^2}{4h}\right) - \mathbf{K}_{4,5}\right] \end{aligned} \tag{44c}$$

As for the masses, the following equations provide terms of the LPM mass matrix

$$m_x = \mathbf{M}_{4,4} - \left(\mathbf{M}_{2,2} - \frac{2\mathbf{M}_{2,3}}{h_c}\right)\left(\frac{h_f}{h} + 1\right) - m_f\left(\frac{h_f}{2h} + 1\right) + \frac{\mathbf{M}_{4,5}}{h} \tag{45a}$$

$$m_{hx} = \left(\mathbf{M}_{2,2} - \frac{2\mathbf{M}_{2,3}}{h_c}\right)\frac{h_f}{h} + m_f\frac{h_f}{2h} - \frac{\mathbf{M}_{4,5}}{h} \tag{45b}$$

$$I_y = \mathbf{M}_{5,5} - \left(\mathbf{M}_{2,2} - \frac{2\mathbf{M}_{2,3}}{h_c}\right)\left(h_f h + h_f^2\right) - m_f\left(\frac{h_f h}{2} + \frac{h_f^2}{4}\right) + \mathbf{M}_{4,5}h \tag{45c}$$

It should be remarked that the geometric parameter *h* of the LPM can be chosen almost arbitrarily [33]. Finally, the damping coefficients deserve some considerations. It was assumed that the overall damping matrix of the soil-foundation-pier system is the sum of the LMP damping matrix and the superstructure damping matrix, the latter expressed as a combination of the stiffness and mass matrices of the superstructure, according to a Rayleigh approach. In this sense, coefficients α and β can be determined considering the damping ratios and frequencies obtained from the identification procedure. In detail, for the *i*-th mode it results

$$\omega_i = |\lambda_i| \tag{46a}$$

$$\xi_i = -\frac{\mathrm{Re}(\lambda_i)}{\omega_i} \tag{46b}$$

As an example, the first two modes can be considered for the calibration of the Rayleigh coefficients. Finally, once the Rayleigh coefficients are estimated, the superstructure contribution to the damping matrix can be estimated and the following equations can be exploited for computing the expected damping coefficients of the LPM:

$$c_x = \mathbf{C}_{4,4} + \frac{\mathbf{C}_{4,5}}{h} - \frac{\alpha}{h}\left[\left(\mathbf{M}_{2,2} - \frac{2}{h_c}\mathbf{M}_{2,3}\right)(h_f + h) + m_f\left(\frac{h_f}{2} + h\right)\right] - \frac{\beta}{h}\left(\mathbf{K}_{2,2} - \mathbf{K}_{1,1}\right)\left(h_f + \frac{h_p}{2} + h\right) \tag{47a}$$

$$c_{hx} = \frac{\alpha}{h}\left[\left(\mathbf{M}_{2,2} - \frac{2}{h_c}\mathbf{M}_{2,3}\right)h_f + m_f\frac{h_f}{2}\right] + \frac{\beta}{h}\left(\mathbf{K}_{2,2} - \mathbf{K}_{1,1}\right)\left(h_f + \frac{h_p}{2}\right) - \frac{\mathbf{C}_{4,5}}{h} \tag{47b}$$

$$c_{ry} = \mathbf{C}_{5,5} + \mathbf{C}_{4,5}h - \alpha h\left[\left(\mathbf{M}_{2,2} - \frac{2}{h_c}\mathbf{M}_{2,3}\right)\left(h_f + \frac{h_f^2}{h}\right) + m_f\left(\frac{h_f}{2} + \frac{h_f^2}{4h}\right)\right] - \beta h\left[\left(\mathbf{K}_{2,2} - \mathbf{K}_{1,1}\right)\left(h_f + \frac{h_p}{2} + \frac{h_f^2}{h} + \frac{h_p h_f}{h}\right) + \frac{\mathbf{K}_{3,3}}{h} + \mathbf{K}_{1,3}\left(\frac{h_c}{h} + \frac{h_d}{h}\right)\right] \tag{47c}$$

2.5 Suggested test procedures and analytical steps

In this section, tests procedures that allow the application of the proposed identification methodology are briefly discussed; both FVTs and AVTs are considered and the necessary experimental and numerical steps are listed in, up to the identification of the stiffness, mass and damping properties of system. In addition, a flowchart of the test procedures and of the analytical steps is reported in Figure 3 to summarise the operational steps.

For FVTs, the following steps apply:

1. perform FVTs using an exciter (i.e. a vibrodyne) and measure accelerations in the transverse direction in a sufficient number of points in order to calculate the experimental signals corresponding to the degrees of freedom of the hypothesised analytical interpretative model. The

vibrodyne can be easily positioned at the deck level (or at the foundation level if the foundation cap is located above the ground level) in order to excite the system in the transverse direction with a sinusoidal sweep signal including all the expected system resonance frequencies;

2. perform an input-output identification of the discrete-time state-space model through procedures available in the literature (e.g. subspace methods [24]) to compute matrices $\mathbf{A}_d$, $\mathbf{B}_d$, $\mathbf{D}_d$ by assuming a model order consistent with that of the analytical system;
3. convert the discrete-time state-space model into a continuous-time state-space model [36] to get matrices ($\mathbf{A}_r$, $\mathbf{B}_r$, $\mathbf{D}_r$). This is possible avoiding aliasing if a sufficiently small time step is assumed; suitable functions implemented in codes such as Matlab [43] can be used;
4. compute the transformation $\mathbf{T}$ according to equation (32) and evaluate the continuous-time state-space model in physical coordinates ($\mathbf{A}_{ph}$, $\mathbf{B}_{ph}$, $\mathbf{D}_{ph}$);
5. solve system (37) in the least square sense to evaluate matrices $\mathbf{M}$, $\mathbf{K}$ and $\mathbf{C}$. It is worth noting that in this case it is not necessary to assume the deck mass m_d to be known;
6. compute the stiffness, mass and damping parameters of the system following equations of Section 2.4 assuming geometric parameters and the foundation mass m_f to be known.

For AVTs, the following steps apply if the noise exciting the structure is measured:

1. perform AVTs measuring accelerations in the transverse direction in a sufficient number of points in order to evaluate signals relevant to the degrees of freedom of the analytical model. Tests include the measure of the noise at the foundation level in terms of accelerations; this can be done for example through geophones.
2. perform an input-output identification of the discrete-time state-space model to compute matrices $\mathbf{A}_d$, $\mathbf{B}_d$, $\mathbf{D}_d$ assuming a model order consistent with that of the analytical system;
3. convert the discrete-time state-space model into a continuous-time state-space model ($\mathbf{A}_r$, $\mathbf{B}_r$, $\mathbf{D}_r$);
4. compute the transformation $\mathbf{T}$ according to equation (32) and evaluate the continuous-time state-space model in physical coordinates ($\mathbf{A}_{ph}$, $\mathbf{B}_{ph}$, $\mathbf{D}_{ph}$);

5. solve system (40) in the least square sense to evaluate matrices **M**, **K** and **C** by assuming the deck mass m_d to be known;
6. compute the stiffness, mass and damping parameters of the system following equations of Section 2.4 assuming geometric parameters and the foundation mass m_f to be known.

For AVTs, the following steps apply if the noise exciting the structure is not measured:

1. perform AVTs and measure accelerations in the transverse direction in a sufficient number of points in order to evaluate signals relevant to the degrees of freedom of the analytical model. Repeat tests by adding a known mass Δm at the deck level, sufficiently small (e.g. 5% of the total mass of the deck) to avoid modification of the mode shapes but to produce a change in poles between the original structure and the loaded-one [21]. Partially or fully loaded trucks can be used as added masses on the deck;
2. perform Operational Modal Analyses (OMAs) of the original structure and the loaded one, evaluating the modal parameters (e.g. resonance frequencies and mode shapes) of the original structure and the change in poles due to the added masses;
3. estimate the scaling factors γ of modes that allows obtaining the mass normalised mode shapes from the un-scaled ones [21];
4. compute the receptance matrix $\mathbf{H}(\omega)$ exploiting equations (27) and (28) and finally evaluate the input noise $\mathbf{F}(\omega)$ in the frequency domain through equation (29) at each degree of freedom of the system. The relevant noise in the time domain can be obtained through an Inverse Fourier Transform.
5. perform an input-output identification of the discrete-time state-space model to compute matrices $\mathbf{A}_d$, $\mathbf{B}_d$, $\mathbf{D}_d$;
6. convert the discrete-time state-space model into a continuous-time state-space model ($\mathbf{A}_r$, $\mathbf{B}_r$, $\mathbf{D}_r$);
7. compute the transformation **T** according to equation (32) and evaluate the continuous-time state-space model in physical coordinates ($\mathbf{A}_{ph}$, $\mathbf{B}_{ph}$, $\mathbf{D}_{ph}$);

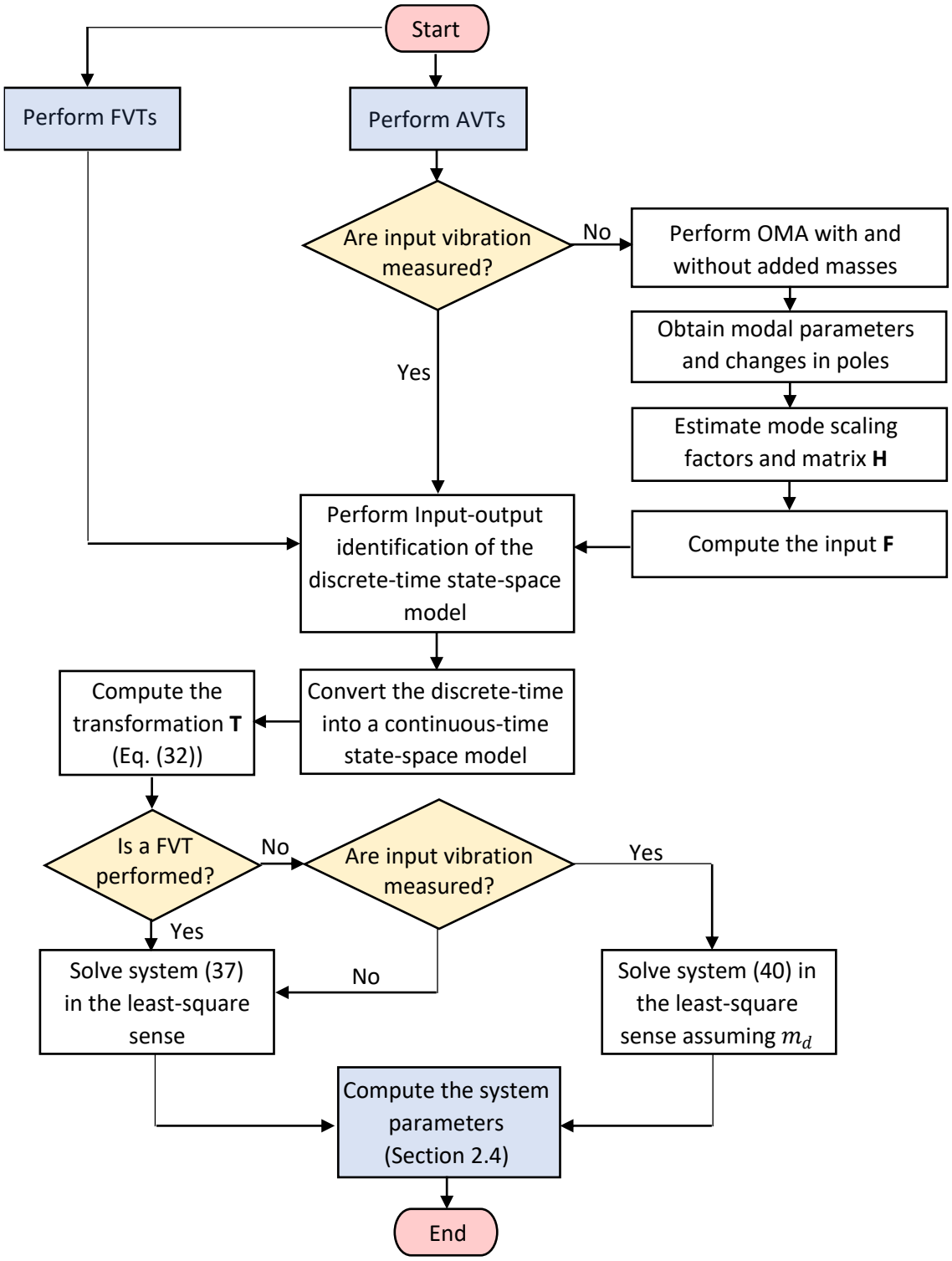

Figure 3. Flowchart of the test procedures.

8. solve system (37) in the least square sense to evaluate matrices **M**, **K** and **C**. It is worth noting that in this case it is not necessary to assume the deck mass m_d to be known since forces acting on each degree of freedom are estimated. The latter are due to all the sources of the ambient excitation (e.g. tremors, human activities, traffic, wind);

9. compute the stiffness, mass and damping parameters of the system following equations of Section 2.4 assuming geometric parameters and the foundation mass m_f to be known.

3 Numerical illustration of the proposed methodology

This section presents some applications to show the potentials of the methodology. Before the methodology can be applied to real case studies, a validation is proposed starting from the analysis of a known system. To this purpose, the model presented in section 2.1 is used, assuming the parameters reported in Table 1. Data are consistent with a steel-concrete twin girder bridge deck with span length of 25 m and 10 m high reinforced concrete piers of diameter 2 m. The concrete material has a Young's modulus E_b = 30000 MPa, a Poisson's ratio ν_b = 0.2 and a density ρ_b = 2.5 t/m^3. As for the soil-foundation system, the LPM parameters are evaluated according to formulas proposed by Carbonari et al. [33] by considering a 3x3 reinforced concrete pile group of length L = 20 m and diameter d = 1 m, equally spaced of $s = 3d$. The pile material has a density ρ_p = 2.5 t/m^3, a Poisson's ratio ν_p = 0.2, and a Young's modulus E_p = 30000 MPa. The foundation mass is obtained from an estimated geometry, which complies with the pile layout. The soil deposit is assumed to be homogenous, with a density ρ_s = 1.8 t/m^3 and a shear wave velocity V_s = 250 m/s. Parameters of the LPM are also reported in Table 1.

The mass, stiffness and damping matrices of the system are reported below; the latter is obtained according to equation (6), calibrating coefficients $\alpha = 0.6797$ and $\beta = 0.002$ considering a 5% damping ratio for the first (1.2942 Hz) and second (6.9695 Hz) resonance frequencies of the undamped system.

$$\mathbf{M} = \begin{bmatrix} 300 & 0 & 0 & 0 & 0 \\ & 129.25 & 81 & 0 & 0 \\ & & 72.9 & 0 & 0 \\ & sym & & 353.73 & 214.18 \\ & & & & 4100.8 \end{bmatrix} \tag{48a}$$

$$\mathbf{K} = \begin{bmatrix} 1e5 & -1e5 & -3e5 & 0 & 0 \\ & 3.618e5 & -1.009e6 & -2.618e5 & -1.8326e6 \\ & & 9.8012e6 & 1.3090e6 & 6.8068e6 \\ & sym & & 1.2173e6 & 1.7201e6 \\ & & & & 1.3855e8 \end{bmatrix} \quad (48b)$$

$$\mathbf{C} = \begin{bmatrix} 404.0131 & -200.1020 & -600.3060 & 0 & 0 \\ & 811.8195 & -1.9640e3 & -523.8658 & -3.6671e3 \\ & & 1.9662e4 & 2.6193e3 & 1.3621e4 \\ & sym & & 5.4365e4 & -4.3993e4 \\ & & & & 6.7241e5 \end{bmatrix} \quad (48c)$$

Table 1. Parameters of the validation model (see Figure 1)

Bridge parameter	Value	Soil & Foundation parameters	Value	LPM parameter	Value
m_d	300 t	Pile layout	3x3	m_x	157.32 t
m_c	90 t	L	20 m	m_{hx}	7.16 t
m_p	78.5 t	d	1 m	I_y	3765.13 tm^2
m_f	150 t	s	3 m	h	2 m
h_d	1.2 m	E_p	30000 MPa	k_x	8.993e5 kN/m
h_c	1.8 m	ν_p	0.2	k_{ry}	1.231e8 kNm/rad
h_p	10 m	ρ_p	2.5 t/m^3	k_{hx}	56250 kN/m
h_f	2 m	ρ_s	1.8 t/m^3	c_x	29804.95 kNs/m
k	1e5 kN/m	V_s	250 m/s	c_{ry}	546190.31 kNms/rad
E_b	30000 MPa			c_{hx}	23907.51 kNs/m
ν_b	0.2				
ρ_b	2.5 t/m^3				

The pier stiffness matrix $\mathbf{K}_p$ is

$$\mathbf{K}_p = \begin{bmatrix} 2.6180e5 & -1.3090e6 & -2.6180e5 & -1.3090e6 \\ & 8.9012e6 & 1.3090e6 & 4.1888e6 \\ & & 2.6180e5 & 1.3090e6 \\ sym & & & 8.9012e6 \end{bmatrix} \quad (49)$$

while non-null or identity components of matrix $\mathbf{A}_c$ (equation 15a) assume the form

$$-\mathbf{M}^{-1}\mathbf{K} = \begin{bmatrix} -333.33 & 333.33 & 1e3 & 0 & 0 \\ -5.9448e3 & -3.7781e4 & 3.0316e5 & 4.3726e4 & 2.3938e5 \\ 1.0721e4 & 5.5820e4 & -4.7130e5 & -6.6540e4 & -3.5935e5 \\ 0 & 484.8562 & -2.7835e3 & -3.2916e3 & 1.6104e4 \\ 0 & 421.5670 & -1.5145e3 & -247.5406 & -3.4628e4 \end{bmatrix} \quad (50a)$$

$$-\mathbf{M}^{-1}\mathbf{C} = \begin{bmatrix} -1.3467 & 0.6770 & 2.0010 & 0 & 0 \\ -11.8957 & -76.2804 & 606.6377 & 87.4963 & 479.0054 \\ 21.4521 & 111.6965 & -943.7525 & -133.1486 & -719.0665 \\ 0 & 0.9702 & -5.5699 & -165.4174 & 230.9553 \\ 0 & 0.8436 & -3.0305 & 19.3675 & -176.0350 \end{bmatrix} \quad (50b)$$

Eigenvalues of matrix $\mathbf{A}_c$ (i.e. of the SFP system) are (equations 22b)

$$\mathbf{\Lambda} = \text{diag}\begin{bmatrix} -0.4486 - j8.1190 \\ -2.6839 - j43.7082 \\ -78.714 - j148.36 \\ -509.83 - j499.17 \\ -0.4486 + j8.1190 \\ -2.6839 + j43.7082 \\ -78.714 + j148.36 \\ -509.83 + j499.17 \\ -20.8814 \\ -158.61 \end{bmatrix} \quad (51)$$

As can be observed from the eigenvalues of equation (51), the soil-foundation-pier system is characterised by four under-damped vibration modes and one over-damped mode, which is not an oscillatory sub-system and will be omitted from the subsequent representations.

Figure 4 shows the real parts (i.e. for phase angle = 0) of the under-damped mode shapes for the selected case study while Figure 5 shows the relevant complexity plots with the corresponding values of the Modal Complexity Factor (MCF) [24]. Each mode in Figure 4 is firstly normalised to get a unitary absolute value of the higher displacement modal component and then scaled for representation issues; the adopted Scale Factor (SF) for each mode is also included in the figure. The first mode is mainly translational with the deck, the pier cap and the foundation vibrating almost in phase (as documented by the very low MCF). Also, the second mode is mainly translational but presents a more important contribution due to the foundation translation and rotation, which lead to an increase of the MCF as a consequence of the non-classically damped soil-foundation system. In addition, the deck and the substructure oscillate in opposite directions.

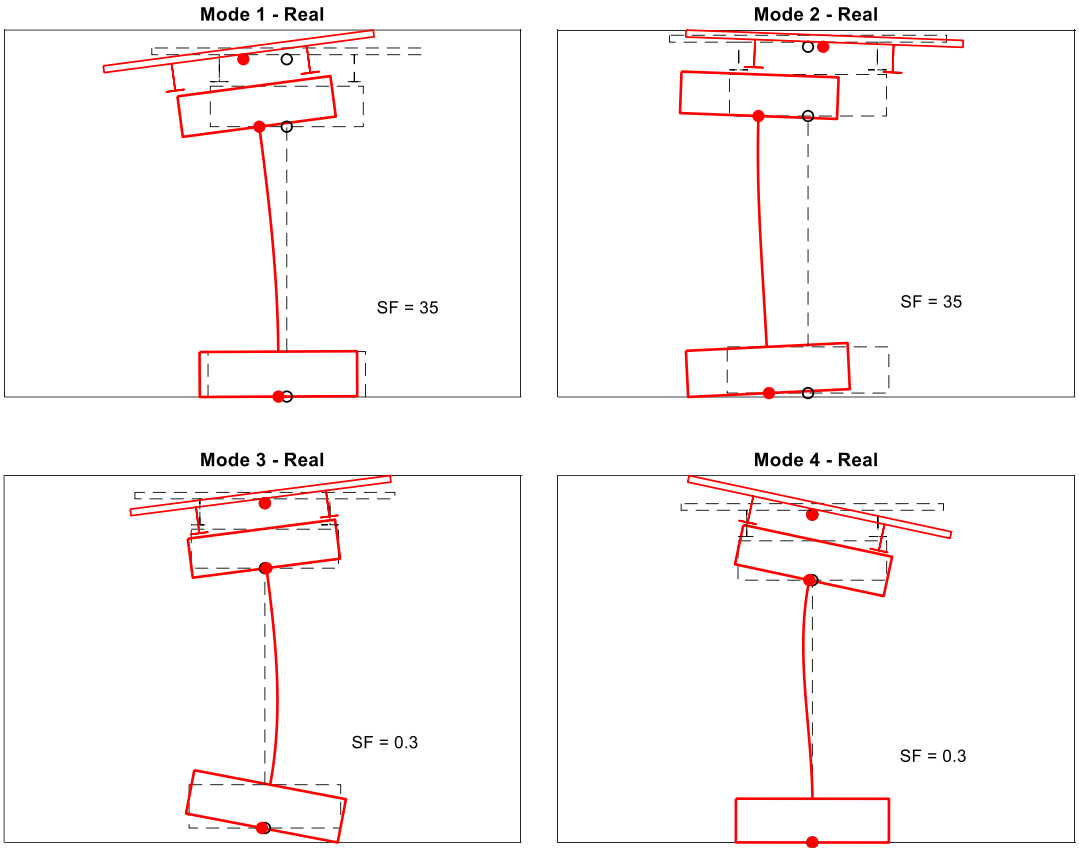

Figure 4. Shape of the under-damped modes.

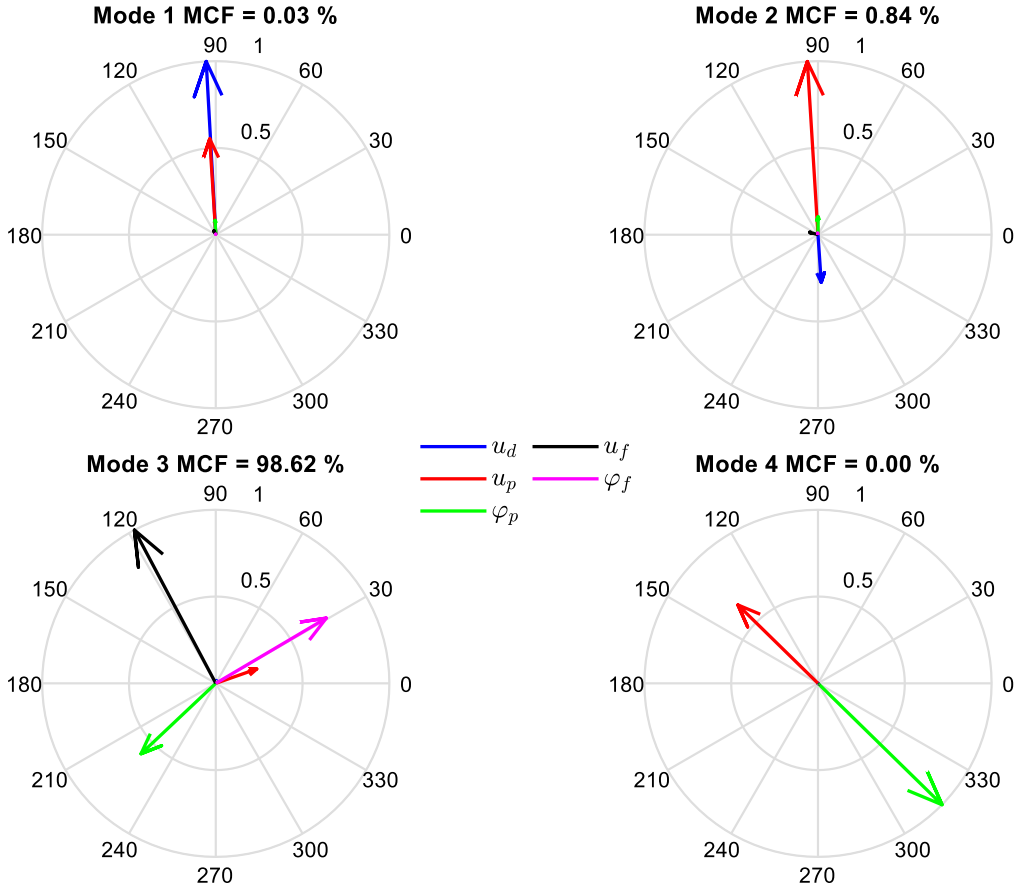

Figure 5. Complexity plots and Mode Complexity Factors (MCFs).

Modes 3 and 4 mainly involve the rotational degrees of freedom; while Mode 4 is mainly characterised by the rotation of the pier cap, with the foundation almost undeformed, Mode 3 is characterised by rotations of both the pier cap and the pile cap. Consequently, taking into account that the non-classically damped nature of the system is only located in the soil-foundation system, MCF of Mode 4 is null and MCF of Mode 3 is the higher one.

Two kinds of input-output dynamic identification test are simulated and the system responses, obtained numerically through the discrete-time state-space model of the SFP system, are assumed to be the measured responses from the corresponding real tests. In detail, a FVT and an AVT are simulated, the latter assuming that the input noise at the foundation level is measured in terms of accelerations.

The FVT is simulated by applying a dynamic force similar to that generated by a vibrodyne at the deck level in the transverse direction of the SFP system. In order to excite all the system vibration modes a frequency sweep from 0.1 to 250 Hz is considered and the force intensity is defined taking into account the performance of real vibrodynes for which a quadratic dependence exists between the force and the angular velocity of the rotating masses. Figure 6a shows the first 5 seconds of the force time history used for the applications while Figure 6b shows the Short Time Fourier Transform of the complete signal, which has a duration of 40 seconds and a frequency content that varies linearly with time from 0.1 Hz to 250 Hz. The AVT is simulated considering that the SFP system is only excited by the ground accelerations $\ddot{u}_g$ that is assumed to be a white Gaussian noise; the latter is considered to be measurable through the use of geophones. Figure 7a shows the first 0.5 seconds of the acceleration time history used for the applications while Figure 7b shows, for the sake of completeness, the Short Time Fourier Transform of the full signal, which has a duration of 50 seconds and a flat spectrum within 0.1 Hz and 300 Hz. A sampling frequency of 500 Hz is assumed.

Figure 8 shows with a thick black line the first 5 seconds of the time histories of accelerations measured at the SFP degrees of freedom obtained from the FVT simulation, while Figure 9 shows, with the same kind of line, the system response obtained from the simulation of the AVT.

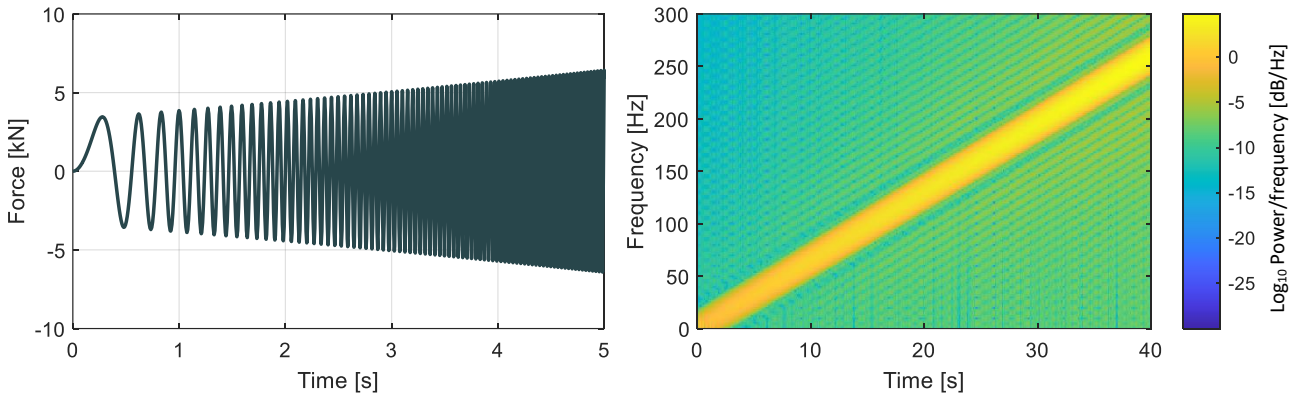

(a) (b)

Figure 6. (a) First 5 s of the input force at the deck level and (b) time-frequency analysis of the whole input force.

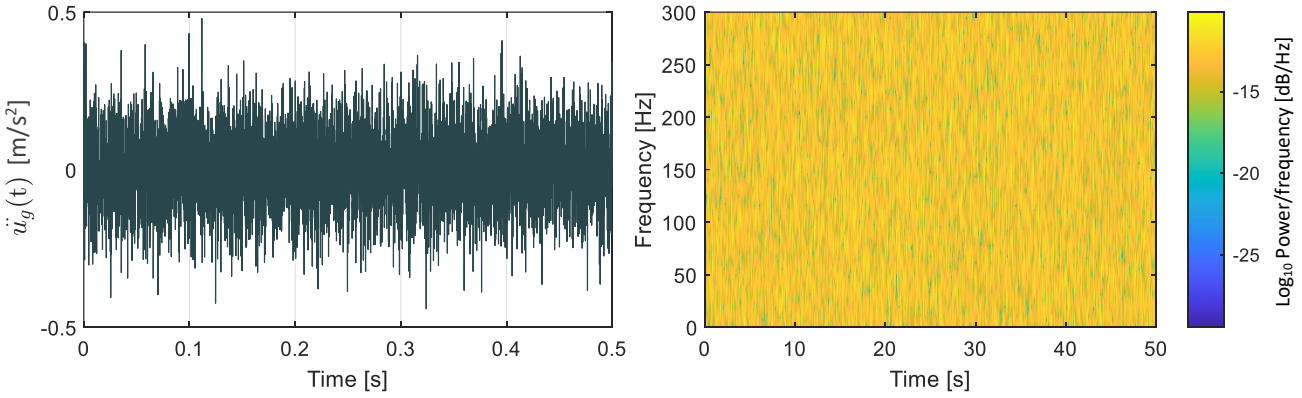

(a) (b)

Figure 7. (a) First 0.5 s of the input acceleration at the ground level and (b) time-frequency analysis of the whole input acceleration.

Starting from the analytical (i.e. measured) response, a deterministic subspace identification procedure from Van Overschee and De Moor (N4SID algorithm) [24] is adopted for the system identification. The response of the identified systems to the measured excitations are shown with thin red lines in Figure 8 and Figure 9, where a perfect matching of the measured and identified responses can be observed.

Steps described in Section 2.5 are adopted to finally obtain the physical parameters of the SFP system starting from the discrete-time identified state-space model. In the sequel, consistency between the known and the identified systems are shown in terms of physical parameters and through the MACX criterion, which is an extension of the Modal Assurance Criterion (MAC) to complex eigenvectors [44]. Components of the continuous-time state-space model in physical coordinates, as well as the identified mass, stiffness and damping matrices, and the SFP system eigenvalues obtained from both the simulated tests are reported in Appendix A.

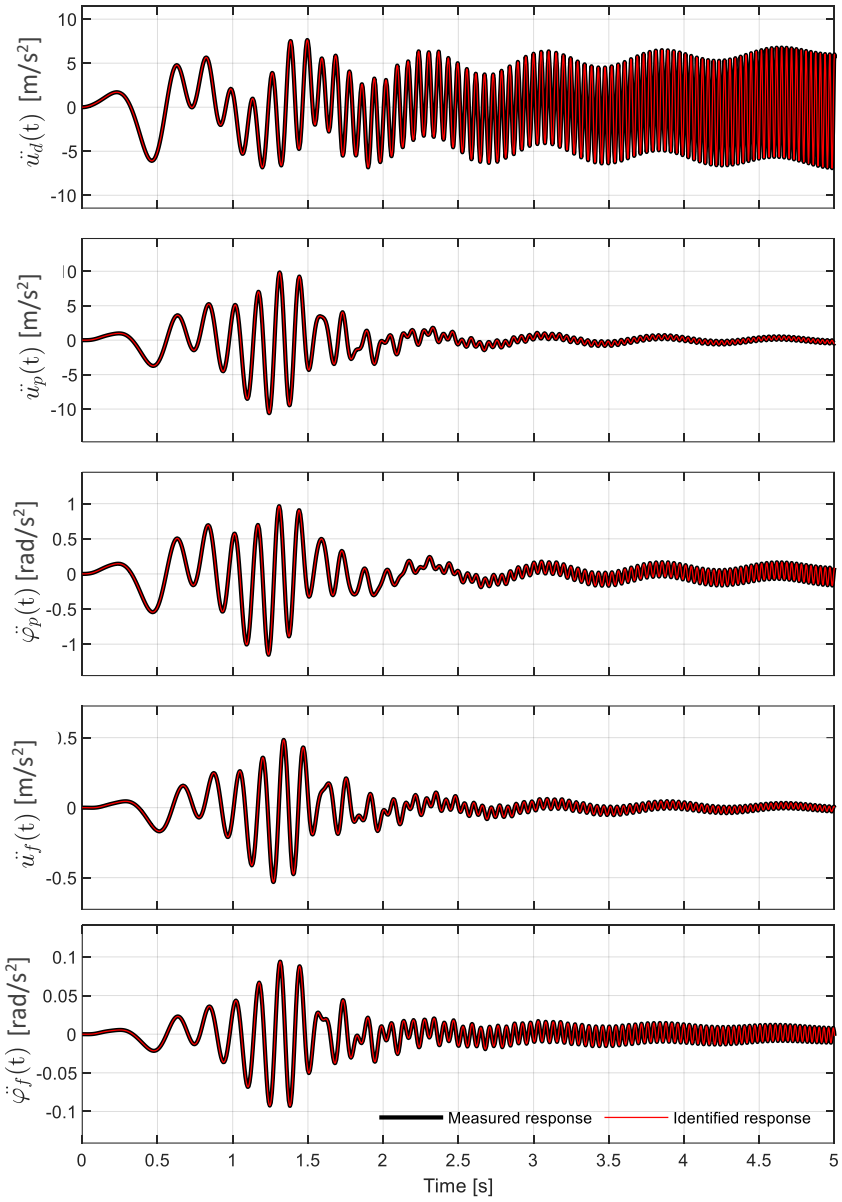

Figure 8. Response of the known and identified systems subjected to a sinusoidal sweep force at the bridge deck level.

Table 2 shows the physical parameters of the SFP system identified from the two simulated tests, together with the relevant percentage errors with respect to the known system. As already mentioned, the approach assumes the geometric parameters to be known, including the LPM rigid link length (that can be assumed in an almost arbitrary manner without influencing the frequency-dependent soil-foundation impedance functions [33]); obviously, for the present applications a value equal to that assumed for the case study is selected in order to make comparisons of the LPM parameters meaningful.

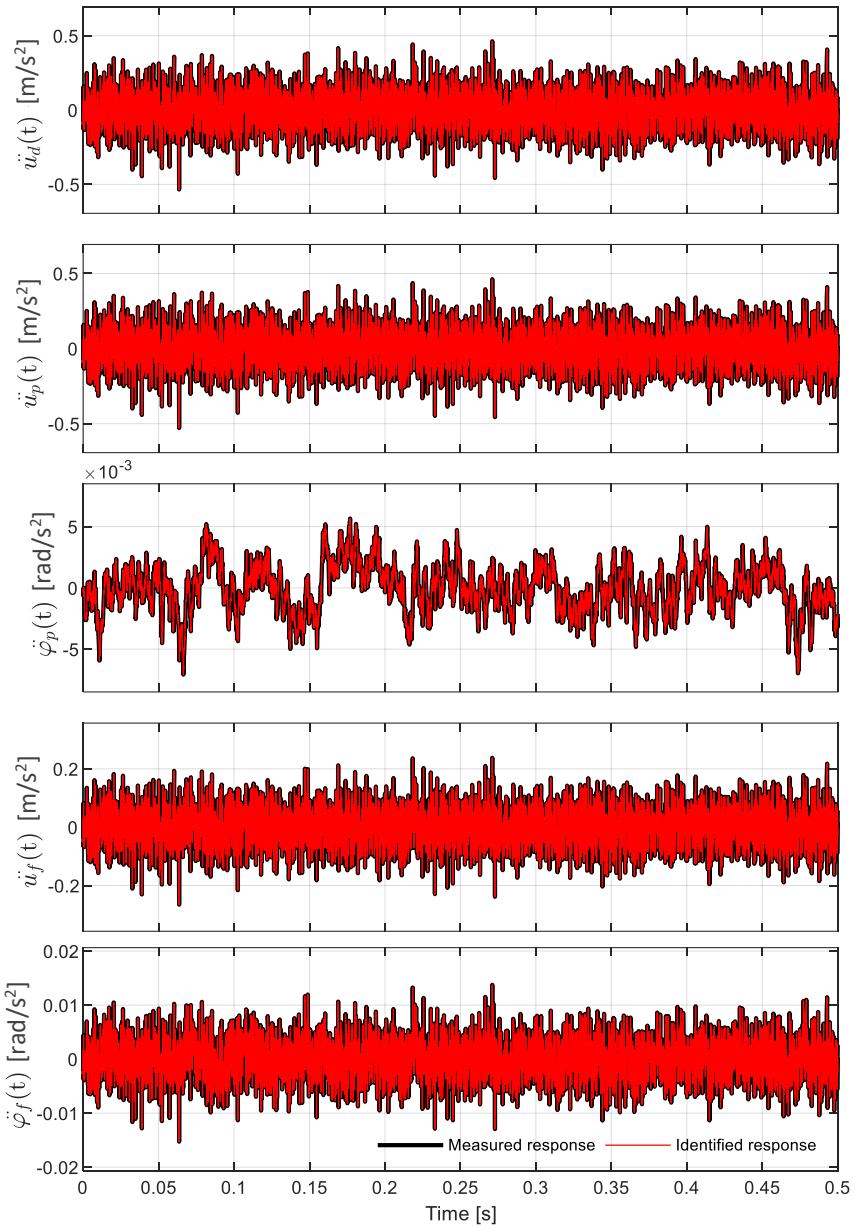

Figure 9. Response of the known and identified system subjected to a noisy ground acceleration.

Furthermore, the foundation mass $m_f = 150$ t is assumed to be known and, for the simulated AVT, also the deck mass $m_d = 300$ t must be imposed to derive the remaining parameters.

Percentage errors of the estimated physical parameters are always very low and practically negligible for values obtained from the simulated FVT. It is worth mentioning that the evaluation of the damping parameters of the LPM requires the estimation of parameters α and β that allow simulating the damping of the superstructure according to a Rayleigh approach; the latter are obtained starting from the first two identified resonance frequencies and damping ratios obtained from Equations (46). The system

eigenvalues (and the relevant eigenvectors) are those of matrix $\mathbf{A}_{ph}$. In detail, the identified frequencies from the simulated FVT and AVT are practically the same and equal to 1.2942 Hz and 6.9695 Hz, while the relevant identified damping ratios are 5.5% and 6.13%, respectively.

Table 2. Comparison between known and identified parameters

		Simulated FVT		Simulated AVT	
Pier parameters	Known value	Identified value	Error [%]	Identified value	Error [%]
m_d [t]	300	299.41	0.20	300	---
m_c [t]	90	89.96	0.05	88.80	1.33
m_p [t]	78.5	78.48	0.03	77.41	1.39
LPM parameters	Known value	Identified value	Error [%]	Identified value	Error [%]
m_x [t]	157.32	157.36	0.02	151.04	3.99
m_{hx} [t]	7.16	7.16	0.04	8.32	16.20
I_y [tm^2]	3765.13	3764.52	0.02	3697.43	1.80
k_x [kN/m]	8.993e5	8.992e5	0.01	8.853e5	1.55
k_{ry} [kNm/rad]	1.231e8	1.231218e8	0.02	1.212076e8	1.54
k_{hx} [kN/m]	56250	56390.04	0.25	54068.66	3.88
c_x [kNs/m]	29804.95	29802.95	0.01	29328.04	1.60
c_{ry} [kNms/rad]	546190.31	546056.95	0.02	537551.07	1.58
c_{hx} [kNs/m]	23907.51	23910.85	0.01	23523.59	1.61

Table 2 only shows mass parameters of the superstructure; the stiffness matrix of the pier obtained from the simulated FVT and AVT are reported below in Equation (52a) and (52b), respectively.

$$\mathbf{K}_p = \begin{bmatrix} 2.61988e5 & -1.31080e6 & -2.61988e5 & -1.31080e6 \\ & 8.91296e6 & 1.31080e6 & 4.19566e6 \\ & & 2.61988e5 & 1.31080e6 \\ sym & & & 8.91296e6 \end{bmatrix} \quad (52a)$$

$$\mathbf{K}_p = \begin{bmatrix} 2.57096e5 & -1.28566e6 & -2.57096e5 & -1.28566e6 \\ & 8.74367e6 & 1.28566e6 & 4.11297e6 \\ & & 2.57096e5 & 1.28566e6 \\ sym & & & 8.74367e6 \end{bmatrix} \quad (52b)$$

With reference to the matrix reported in Equation (49), percentage errors in the range of 0.01-0.16% are observed for the matrix of Equation (52a), obtained from the simulated FVT, and in the range of 1.61-1.78% for the matrix of Equation (52b), resulting from the simulated AVT.

Finally, Figure 10 shows the MACX values [44] obtained by comparing the complex eigen vectors of the known system and the complex eigenvectors of the identified systems; the latter are obtained by solving the eigenvalue problem for the matrixes $\mathbf{A}_{ph}$, whose components are available in Appendix A for both the case of the simulated FVT and AVT. MACX values in Figure 10 demonstrate a very good correlation between the mode shapes of the original system and those of the identified ones. MACX values are also reported in a table format in Figure 11 to highlight that values are practically coincident, with differences only beyond the forth decimal digit. In the same figure, values obtained with the classical MAC criterion are also reported; as can be observed, differences only appear for the third mode, which is characterised by a significant complex nature.

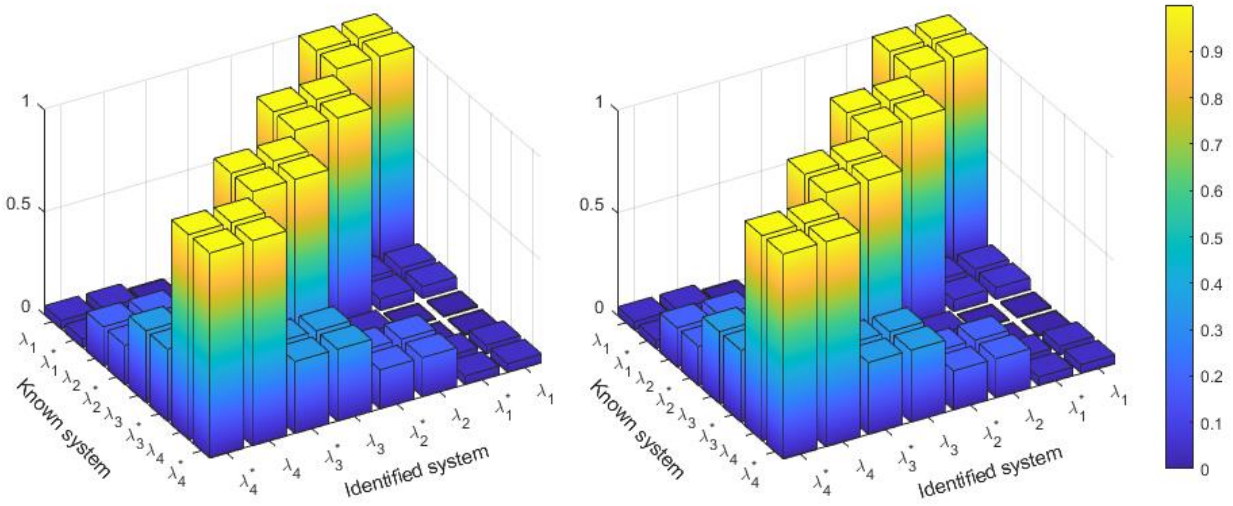

(a) (b)

Figure 10. MACX diagrams between complex eigen vectors of the known system and the eigenvectors identified from (a) the simulated FVT and (b) the simulated AVT

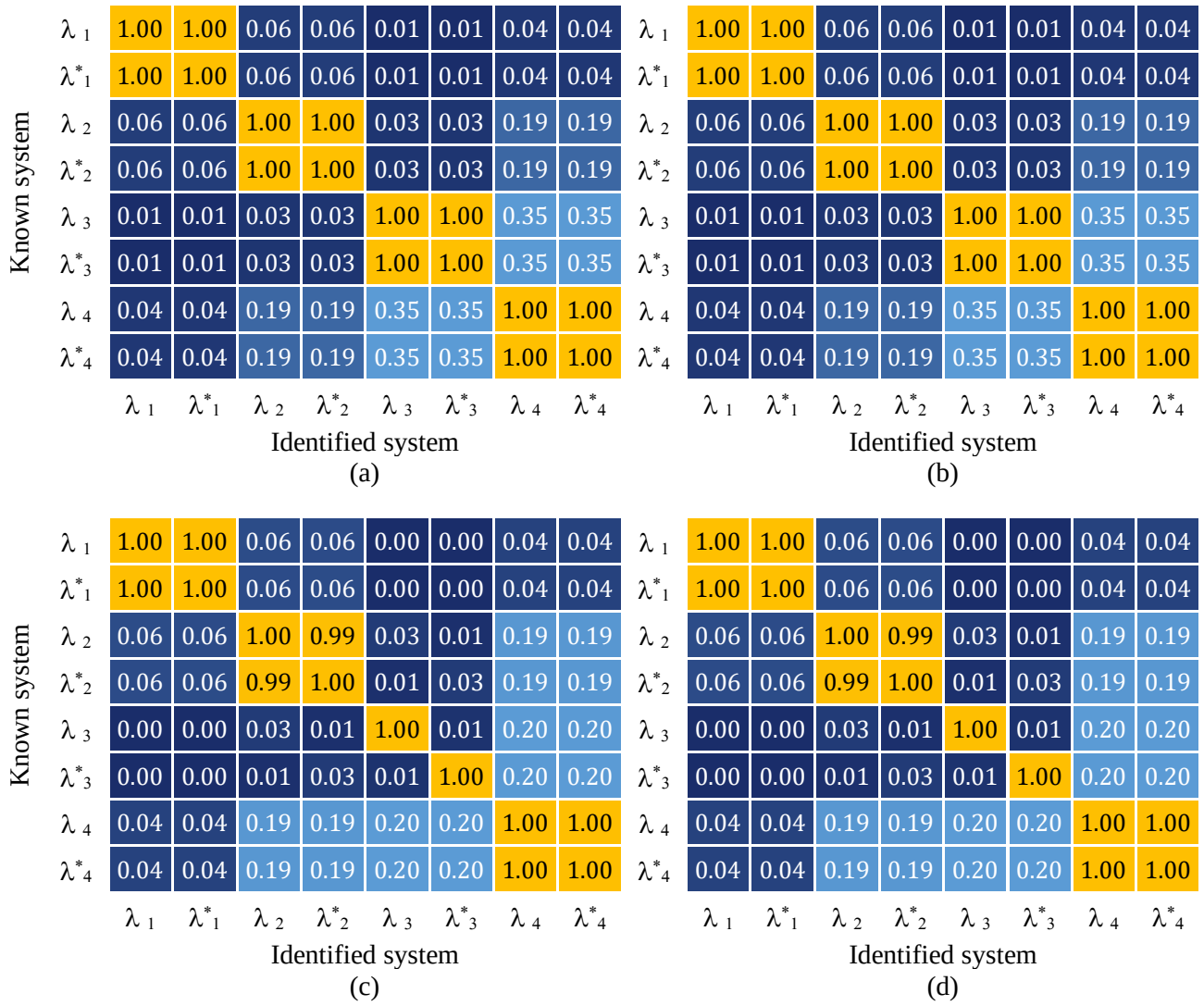

Figure 11. Comparison of eigen vectors (known system and identified one): (a) MACX for to the simulated FVT; (b) MACX for the simulated AVT; (c) MAC for to the simulated FVT; (d) MAC for the simulated AVT

4 Conclusions

A methodology for the identification of the physical parameters of a model describing the transverse dynamics of soil-foundation-pier systems has been presented in this paper. The methodology, which excludes the need of model updating procedures, requires the execution of forced vibration or ambient vibration tests on the real structure that has to be characterised, from which the first-order state-space model can be identified according to well-established procedures available in the literature. The order of the model is assumed to be compliant with that of the developed interpreting model and the state-space model is expressed in the physical coordinates, so that the space vector contains displacements and velocities. Finally, the stiffness, mass and damping matrices of the real system are identified, and

the physical parameters of the numerical model are computed comparing the identified and numerical matrices. The procedure also allows the experimental identification of the parameters of a lumped system able to capture the frequency-dependent behaviour of the soil-foundation system in time domain analysis. The application of the proposed approach is based on the assumption that the system geometric parameters are known (i.e. measurable through in-situ inspections) and on some additional acceptable hypotheses that depend on the executed tests. In detail:

1. if forced vibration tests are executed, all the physical parameters of the numerical model representing the real system can be determined by assuming the foundation mass to be known;
2. for ambient vibration tests in which the noise exciting the structure is measured at the ground level through geophones, the physical parameters of the numerical model can be all estimated by assuming the deck and the foundation masses to be known. In this case, the methodology is based on the assumption that the exciting sources only come from the soil;
3. data from ambient vibration tests can be also adopted without the need of measuring the ground accelerations; in this case, tests must be repeated with masses added on the structure in a suitable configuration that allows the estimation of the scaling factors of the modes determined through the operational modal analyses. The latter can be used to reconstruct the receptance matrix of the system and finally the input exciting the structures at the measured points. In this case, the estimated actions include all the sources of excitation (i.e. ground tremors, wind, traffic).

Laboratory tests and applications of the proposed identification methodology on real bridges are ongoing; results will provide a clear overview of the approach feasibility and the accuracy of results obtained from the different approaches.

Finally, it is worth remarking that the methodology can be also exploited for structural health monitoring and damage identification purposes by simply repeating tests during time and by identifying changes in the physical stiffness matrix of the structure, including the soil-foundation system, where damage cannot be observed directly. Finally, the procedure can be also applied in case of seismic data (e.g. obtained from a monitoring system) if both base and floor accelerations are registered; in this case, if tests

performed before and after the earthquake are available, the presence of damage can be identified and the localization can be attempted.

Appendix A

Components of identified matrixes $\mathbf{A}_{ph}$ from the simulated FVT are

$$-\mathbf{M}^{-1}\mathbf{K} = \begin{bmatrix} -333.3511 & 333.2465 & 1000.6966 & -0.4193 & -3.1686 \\ -5.9448e3 & -3.7781e4 & 3.0316e5 & 4.3726e4 & 2.3938e5 \\ 1.0721e4 & 5.5820e4 & -4.7130e5 & -6.6540e4 & -3.5935e5 \\ -0.0024 & 484.8450 & -2.7835e3 & -3.2914e3 & 1.6104e4 \\ -0.0073 & 421.5479 & -1.5143e3 & -247.4283 & -3.4629e4 \end{bmatrix} \quad \text{(A1a)}$$

$$-\mathbf{M}^{-1}\mathbf{C} = \begin{bmatrix} -1.3467 & 0.6669 & 2.0026 & 0.0152 & -0.0060 \\ -11.8957 & -76.2806 & 606.6391 & 87.5108 & 478.9996 \\ 21.4520 & 111.6964 & -943.7518 & -133.1480 & -719.0661 \\ 0 & 0.9702 & -5.5696 & -165.4121 & 230.9530 \\ 0 & 0.8435 & -3.0302 & 19.3716 & -176.0367 \end{bmatrix} \quad \text{(A1b)}$$

Identified mass, stiffness, and damping matrices from the simulated FVT are

$$\mathbf{M} = \begin{bmatrix} 299.4070 & -0.1449 & -0.0946 & 0.0150 & -0.0481 \\ & 129.1980 & 80.9632 & 0.0090 & -0.0168 \\ & & 72.9030 & 0.0097 & 0.0153 \\ & sym & & 353.7520 & 214.1634 \\ & & & & 4100.1019 \end{bmatrix} \quad \text{(A2a)}$$

$$\mathbf{K} = \begin{bmatrix} 9.9960e4 & -9.9960e4 & -3.0028e5 & 43.3182 & -249.6582 \\ & 3.6195e5 & -1.0105e6 & -2.6200e5 & -1.8337e6 \\ & & 9.8138e6 & 1.3108e6 & 6.8173e6 \\ & sym & & 1.2176e6 & 1.7211e6 \\ & & & & 1.3854e8 \end{bmatrix} \quad \text{(A2b)}$$

$$\mathbf{C} = \begin{bmatrix} 403.5218 & -200.1251 & -600.9333 & -0.0827 & -0.6122 \\ & 812.0902 & -1.9670e3 & -524.2717 & -3.6693e3 \\ & & 1.9687e4 & 2.6229e3 & 1.3642e4 \\ & sym & & 5.4367e4 & -4.3997e4 \\ & & & & 6.7233e5 \end{bmatrix} \quad \text{(A2c)}$$

Eigenvalues obtained from the simulated FVT are

$$\boldsymbol{\Lambda} = \text{diag}\begin{bmatrix} -0.4486 - j8.1190 \\ -2.6839 - j43.7082 \\ -78.714 - j148.36 \\ -509.82 - j499.17 \\ -0.4486 + j8.1190 \\ -2.6839 + j43.7082 \\ -78.714 + j148.36 \\ -509.82 + j499.17 \\ -20.8814 \\ -158.61 \end{bmatrix} \tag{A3}$$

Components of identified matrixes $\mathbf{A}_{ph}$ from the simulated AVT are

$$-\mathbf{M}^{-1}\mathbf{K} = \begin{bmatrix} -333.3333 & 333.3333 & 1000.08 & -0.0486 & 0.1894 \\ -5.9448e3 & -3.7781e4 & 3.0316e5 & 4.3728e4 & 2.3938e5 \\ 1.0721e4 & 5.5820e4 & -4.7129e5 & -6.6544e4 & -3.5934e5 \\ 0 & 484.9290 & -2.7842e3 & -3.2909e3 & 1.6104e4 \\ 0.0105 & 421.5969 & -1.5147e3 & -247.8156 & -3.4628e4 \end{bmatrix} \tag{A4a}$$

$$-\mathbf{M}^{-1}\mathbf{C} = \begin{bmatrix} -1.3470 & 0.6669 & 2.0009 & -0.0004 & 0 \\ -11.8826 & -76.2740 & 606.6415 & 87.5118 & 479.0058 \\ 21.4325 & 111.6869 & -943.7583 & -133.1718 & -719.0671 \\ 0.0041 & 0.9722 & -5.5685 & -165.4124 & 230.9554 \\ 0.0015 & 0.8428 & -3.0305 & 19.3659 & -176.0352 \end{bmatrix} \tag{A4b}$$

Identified mass, stiffness, and damping matrices from the simulated FVT are

$$\mathbf{M} = \begin{bmatrix} 300 & 1.2497 & 0.8132 & 0.1529 & 0.2821 \\ & 127.5143 & 79.9240 & 0.0532 & 0.0817 \\ & & 71.8420 & 0.0291 & 0.0209 \\ & sym & & 348.0815 & 210.7764 \\ & & & & 4035.5563 \end{bmatrix} \tag{A5a}$$

$$\mathbf{K} = \begin{bmatrix} 9.8711e4 & -9.8366e4 & -2.9478e5 & 54.6792 & 313.8934 \\ & 3.5581e5 & -9.9088e5 & -2.5732e5 & -1.8018e6 \\ & & 9.6280e6 & 1.2858e6 & 6.6843e6 \\ & sym & & 1.1973e6 & 1.6915e6 \\ & & & & 1.3634e8 \end{bmatrix} \tag{A5b}$$

$$\mathbf{C} = \begin{bmatrix} 401.5267 & -196.0780 & -588.9484 & -0.8953 & 6.2032 \\ & 798.6054 & -1.9283e3 & -515.3336 & -3.6022e3 \\ & & 1.9315e4 & 2.5719e3 & 1.3373e4 \\ & sym & & 5.3494e4 & -4.3291e4 \\ & & & & 6.6170e5 \end{bmatrix} \tag{A5c}$$

Eigenvalues obtained from the simulated AVT are

$$\boldsymbol{\Lambda} = \text{diag}\begin{bmatrix} -0.4487 - j8.1190 \\ -2.6839 - j43.7081 \\ -78.714 - j148.36 \\ -509.83 - j499.17 \\ -0.4487 + j8.1190 \\ -2.6839 + j43.7081 \\ -78.714 + j148.36 \\ -509.83 + j499.17 \\ -20.8762 \\ -158.61 \end{bmatrix} \tag{A6}$$

References

[1] Rodrigues J, Ledesma M. Modal identification of a viaduct before and after retrofitting works. *Proceedings of 25th Int. Modal Analysis Conference*. 2007. Orlando FL, USA.

[2] Cunha A, Magalhães F, Caetano E. Output-only modal identification of Luiz I bridge before and after rehabilitation. *Proceedings of the International Conference on Noise and Vibration Engng*. 2006. Leuven, Belgium.

[3] Niousha A, Motosaka M. System identification and damage assessment of an existing building before and after retrofit. *Journal of Structural Engineering (Japan)*. 2007;53B:297-304.

[4] Ercan E. Assessing the impact of retrofitting on structural safety in historical buildings via ambient vibration tests. *Construction and Building Materials*. 2018;164:337-349.

[5] Soyoz S, Taciroglu E, Orakcal K, Nigbor R, Skolnik D, Lus H, Safak E. Ambient and forced vibration testing of a reinforced concrete building before and after its seismic retrofitting. *Journal of Structural Engineering*. 2013;139(10):1741-1752.

[6] Gara F, Carbonari S, Roia D, Balducci A, Dezi L. Seismic retrofit assessment of a school building through operational modal analysis and f.e. modelling. *ASCE Journal of Structural Engineering*. 2021;147(1):04020302.

[7] Ceravolo R, Matta E, Quattrone A, Zanotti Fragonara L. Amplitude dependence of equivalent modal parameters in monitored Buildings during earthquake swarms. *Earthquake Engineering & Structural Dynamics*. 2017;46(14):2399-2417.

[8] Ditommaso R, Mucciarelli M, Ponzo FC. Analysis of non-stationary structural systems by using a band-variable filter. *Bulletin of Earthquake Engineering*. 2012;10(3):895-911.

[9] Ghahari SF, Abazarsa F, Ghannad MA, Taciroglu E. Response-Only Modal Identification of Structures Using Strong Motion Data. *Earthquake Engineering & Structural Dynamics*. 2013;42(8):1221-42.

[10] Hu R. Xu Y. SHM-based seismic performance assessment of high-rise buildings under long-period ground motion. *Journal of Structural Engineering*. 2019;145(6):04019038.

[11] O'Reilly GJ, Perrone D, Fox M, Monteiro R, Filiatrault A, Lanese I, Pavese A. System identification and seismic assessment modeling implications for Italian school buildings. *Journal of Performance of Constructed Facilities*. 2019; 33(1):04018089.

[12] Gara F, Arezzo D, Nicoletti V, Carbonari S. Monitoring of the modal properties of a RC school building during the 2016 central Italy seismic swarm. *Journal of Structural Engineering ASCE*. 2021; 147(7): 05021002.

[13] Causevic, MS. Mathematical modelling and full-scale forced vibration testing of a reinforced concrete structure, *Engineering Structures*. 1987; 9: 2-8.

[14] De Sortis A, Antonacci E, Vestroni F. Dynamic identification of a masonry building using forced vibration tests, Engineering Structures, 2005;27:155-165.

[15] Omenzetter P, Beskhyroun S, Shabbir F, Chen GW, Chen X, Wang S, Zha A. Forced and ambient vibration testing of full scale bridges. A report submitted to Earthquake Commission Research Foundation (Project No. UNI/578). October 2013.

[16] Green, MF. Modal test methods for bridges: a review, Proceedings of IMAC XIII:13th International Modal Analysis Conference, 1995;552-558.

[17] Gentile C, Martinez y Cabrera F. Dynamic performance of twin curved cable-stayed bridges, *Earthquake Engineering and Structural Dynamics*, 2004;33:15–34.

[18] Gara F, Regni M, Roia D, Carbonari S, Dezi F. Evidence of coupled soil-structure interaction and site response in continuous viaducts from ambient vibration tests. *Soil Dynamics and Earthquake Engineering*. 2019; 120:408-422.

[19] Agbabian MS, Masri SF, Miller RK, Caughey TK. System identification approach to detection of structural changes. *ASCE Journal of Engineering Mechanics*. 1991;117(2):370-390.

[20] Smyth AW, Pei JS. Integration of measured response signals for nonlinear structural health monitoring. *Proceedings of the third US-Japan workshop on nonlinear system identification and health monitoring*. 2000. Los Angeles, CA.

[21] Parloo P, Verboven P, Guillaume P, Van Overmeire M. Sensitivity-based operational mode shape normalisation. *Mechanical Systems and Signal Processing*. 2002;16(5):757-767.

[22] Heylen W, Lammens S, Sas P. Modal analysis theory and testing. Acco, Leuven, 1997.

[23] Phan MQ, Longman R. Extracting mass, stiffness, and damping matrices from identified state-space models. *Proceedings of the AIAA Guidance, Navigation, and Control Conference and Exhibit*. 2004. Providence, Rhode Island.

[24] Van Overschee P, De Moor B. Subspace identifications for linear systems: theory, implementation and applications. Kluwer, Boston, 1996.

[25] Tseng DH, Longman RW, Juang JN. Identification of the structure of the damping matrix in second order mechanical systems. *Advances in the Astronautical Sciences*. 1994;87:167-190.

[26] Tseng DH, Longman RW, Juang JN. Identification of gyroscopic and nongyroscopic second-order mechanical systems including repeated problems. *Advances in the Astronautical Sciences*. 1994;87:145-165.

[27] Alvin KF, Park KC. Second order structural identification procedure via state-space based system identification. *AIAA Journal*. 1994;32(2):397-406.

[28] De Angelis M, Lus H, Betti R, Longman RW. Extracting physical parameters of mechanical models from identified state-space representatations. *ASME Journal of Applied Mechanics*. 2002;69:617-625.

[29] Gara F, Regni M, Roia D, Carbonari S, Dezi F. Evidence of coupled soil-structure interaction and site response in continuous viaducts from ambient vibration tests. *Soil Dynamics and Earthquake Engineering*. 2019;120:408-422.

[30] Carbonari S, Dezi F, Gara F. The role of soil-structure interaction in the interpretation of dynamic tests on the "Chiaravalle viaduct". *Proceedings of COMPDYN 2019 7th International Conference on Computational Methods in Structural Dynamics and Earthquake Engineering*. 2019;3:4147-4156.

[31] Wolf JP. Soil-structure interaction analysis in time domain. 1988. Prentice-Hall, Englewood Cliffs, N.J.

[32] Taherzadeh R, Clouteau D, Cottereau RC. Simple formulas for the dynamic stiffness of pile groups. *Earthquake Eng. Struct. Dynam*. 2009;38:1665-1685.

[33] Carbonari S, Morici M, Dezi F, Leoni G. A lumped parameter model for time-domain inertial soil-structure interaction analysis of structures on pile foundations.

[34] Morici M, Minnucci L, Carbonari S, Dezi F, Leoni G. Simple formulas for estimating a lumped parameter model to reproduce impedances of end-bearing pile foundations. *Soil Dynamics and Earthquake Engineering*. 2019;121:341-355. *Earthquake Eng. Struct. Dynam*. 2018;47(11):2147-2171.

[35] Wolf JP. Foundation Vibration Analysis using Simple Physical Models 1994. Prentice-Hall, Englewood Cliffs, N.J.

[36] Peeters B. System Identification and Damage Detection in Civil Engineering. Ph.D. Thesis. Faculteit Toegepaste Wetenschappen Department Burgerlijke Bouwkinde. Katholieke Universiteit Leuven.

[37] Makris N, Badoni D, Delis E, Gazetas G. Prediction of observed bridge response with soil-pile-structure interaction. *ASCE Journal of Structural* Engineering. 1994;120(10):2992-11.

[38] Ciampoli M, Pinto PE. Effects of soil-structure interaction on inelastic seismic response of bridge piers. *ASCE Journal of Structural Engineering*. 2005;121(5):806-14.

[39] Sextos AG, Pitilakis KD, Kappos AJ. Inelastic dynamic analysis of RC bridges accounting for spatial variability of ground motion, site effects and soil-structure interaction phenomena. Part 2: Parametric study. *Earthquake Engineering and Structural Dynamics*. 2003;32:629-52.

[40] Carbonari S, Morici M, Dezi F, Gara F, Leoni G. Soil-structure interaction effects in single bridge piers founded on inclined pile groups. *Soil Dynamics and Earthquake Engineering*. 2017;92:52-67.

[41] González F, Padrón LA, Carbonari S, Morici M, Aznárez JJ, Dezi F, Leoni G. Seismic response of bridge piers on pile groups for different soil damping models and lumped parameter representations of the foundation. *Earthquake Engineering and Structural Dynamics*. 2019;48(3):306-327.

[42] Capatti MC, Tropeano G, Morici M, Carbonari S, Dezi F, Leoni G, Silvestri F. Implications of non-synchronous excitation induced by nonlinear site amplification and soil-structure interaction on the seismic response of multi-span bridges founded on piles. *Bulletin of Earthquake Engineering*. 2017;15(11):4963-4995.

[43] MATLAB, 2020b. Natick, Massachusetts: The MathWorks Inc.

[44] Vacher P, Jacquier B, Bucharles A. Extensions of the MAC criterion to complex modes. Proceedings of the ISMA2010-USD2010 24th International Conference on Noise and Vibration Engineering: 2713-2726